REVIEW

Transformation of peptides to small molecules in medicinal chemistry: Challenges and opportunities

Zeyu Han [a,b], **Zekai Shen** [a,b], **Jiayue Pei** [a,b], **Qidong You** [a,b,*], **Qiuyue Zhang** [a,b,*], **Lei Wang** [a,b,*]

[a]*State Key Laboratory of Natural Medicines and Jiangsu Key Laboratory of Drug Design and Optimization, China Pharmaceutical University, Nanjing 210009, China*
[b]*Department of Medicinal Chemistry, School of Pharmacy, China Pharmaceutical University, Nanjing 210009, China*

Abstract   Peptides are native binders involved in numerous physiological life procedures, such as cellular signaling, and serve as ready-made regulators of biochemical processes. Meanwhile, small molecules compose many drugs owing to their outstanding advantages of physiochemical properties and synthetic convenience. A novel field of research is converting peptides into small molecules, providing a convenient portable solution for drug design or peptidomic research. Endowing properties of peptides onto small molecules can evolutionarily combine the advantages of both moieties and improve the biological druggability of molecules. Herein, we present eight representative recent cases in this conversion and elaborate on the transformation process of each case. We discuss the innovative technological methods and research approaches involved, and analyze the applicability conditions of the approaches and methods in each case, guiding further modifications of peptides to small molecules. Finally, based on the aforementioned cases, we summarize a general procedure for peptide-to-small molecule modifications, listing the technological methods available for each transformation step and providing our insights on the applicable scenarios for these methods. This review aims to present the progress of peptide-to-small molecule modifications and propose our thoughts and perspectives for future research in this field.

*Corresponding authors.
    E-mail addresses: youqd@163.com (Qidong You), zhangqiuyue_1994@163.com (Qiuyue Zhang), leiwang.91@cpu.edu.cn (Lei Wang).

1. Introduction

Small molecules are acknowledged as the mainstream of drug development, while drugs are found in a complex variety of sources. Obtaining them through peptide modification is important for small-molecule drug development. Peptides are commonly known for their high selectivity and efficacy, considerable safety, and good tolerance[1]. Considering the outstanding advantages of peptides, they have fixed ways to synthesize, are available for modification and optimization, are less prone to degradation compared to exogenous compounds, etc.[2−6]. As a result of enhanced membrane permeability, bioavailability, and absorption, they are prone to exhibit therapeutic effects *in vivo*[7,8]. The discovery of peptides is mostly based on endogenous interactions and is easily accessible through rational drug design approaches. Peptides have naturally outstanding bioavailability and absorption *in vivo*, however when used as oral drugs, deficiencies of peptides reveal poor metabolic stability, limited oral administration, and low membrane permeability[9,10]. Therefore, structural modification of peptides to retain the active pharmacophore and slim down to small molecules is very necessary and is one of the popular approaches for small molecule drug development[11−14].

The classic angiotensin-converting enzyme inhibitor, captopril, was obtained by modifying teprotide extracted from snake venom, which was regarded as the first successful case of peptide modification to a small molecule and was introduced to the market in 1971[15,16]. This breakthrough in drug development from peptides proved that this strategy is reasonable and inspired medicinal chemists worldwide to design small molecules derived from peptides. In the 1990s, Duncia and Smeby et al. designed angiotensin II AT1 antagonists, following the successful workflow inspired by captopril, enabling peptides to be transformed into small molecules in a highly rational way[17,18]. One of the most typical oral small-molecule drugs from peptides approved by the European Medicines Agency is Parecoxib, initially developed as a peptide-based COX-2 inhibitor, transformed into a small molecule by Pfizer to provide effective pain relief with improved pharmacokinetic properties and bioavailability in 2002[19−22]. For years to come, technologies have evolved, and skills and tools for optimization from peptides to small molecules through medicinal chemistry strategies have also developed to the next level. In classical pharmaceutical refinement, small molecules were created by simulating the copy of residues from peptides. In the interval of the optimization, peptidomimetics emerge as the initiatory fusion product and become a potential intermediate field of research on the road to small molecules[23−27]. During the time-consuming and inefficient classical optimization, difficulties appeared occasionally. In many situations, identifying the active target structure required investigating and confirming hundreds to thousands of molecules to find the necessary structures for small molecules to mimic. How can medicinal chemists gain experience from successful cases in optimizing peptides to small molecules have now become a topic of the field.

Optimizing peptides into small molecules has always been a subject worth exploring. The major modification processes commonly begin with locating peptide targets, with a certain standout site to be simulated by a constructed scaffold and substituent groups. Finally, this process results in the superior binding activity compound hit, which is optimized by following structure–activity relationship (SAR) studies to ameliorate its druggability. This "transformation" process can be broadly divided into four stages: transitioning from native peptides to peptidomimetics, slimming down from peptidomimetics to active scaffolds, mimicking secondary conformations from active scaffolds to potential molecules, and conducting SAR studies to arrive at small molecules[28−30]. The transformation of peptides into small molecules presents several challenges. The presence of amino bonds and natural residues in peptides complicates the classical molecular design[31−33]. However, recent advancements in technology and methodology have provided more rational and convenient ways to facilitate this transformation. Key steps in this transformation include eliminating functionally unrelated residues, reducing non-essential scaffold atoms, and preserving crucial interaction sites in peptides. These new approaches have substantially eased the process of peptide-to-small molecule transformation, paving the way for future advancements in this field. In second configurations, novel tech has changed the traditional procedure of drug design in a way of applying virtual simulations instead of physical ones, or completely generate the small molecules in algorithms. As a character of innovation, new technologies and new methods such as database screening, exploring key orientation (EKO) strategy, machine learning (ML), and fingerprint representation are also being produced, providing novel perspectives and ideas to systematically modify peptides into small molecules (Table 1)[34−37]. The general idea is to "transform" existing peptides into small molecules and optimize small molecules using medicinal chemistry strategies. The overall process is likely to be a particular category of "transformation"[12]. Modifying peptides to small molecules is a complex process requiring systematic elaboration to provide scholars with a clear status quo and blueprint. However, how medicinal chemists utilize approaches to achieve the desired small molecular design from peptides remains an open topic. Recently, there have been several successful cases of "transforming" peptides into small molecules with improved design strategies or advanced technologies[38].

This perspective aims to provide an introduction and a summary of cases optimizing peptides into small molecules in our view. We emphatically introduce eight characteristic cases focusing on various fields, emphasizing the classic and novel methods (Table 1). This includes the classical way of step-by-step optimization, protein−protein interface (PPI) key region-guided inhibitor designing, pocket-fitting warhead design, essential amino acid sequence template simplification, database substitution toward core structures, and ML and artificial intelligence (AI)-aided optimization. This method of obtaining small molecules from peptides can be utilized to find novel peptide markers, design small-molecule compounds, identify peptide signaling structures, and build a molecular substituent group library. This approach can also assist in increasing the bio-affinity of small molecules and improving the physicochemical properties of peptides to facilitate the transition of peptidomimetics to drugs. With the intention of quick updates over recent years and anticipating the outlook, we are providing an integrated perspective on the approaches over these years with selected cases below.

2. Classical optimization from peptides to small molecules

2.1. Conventional step-by-step optimization of nicotinamide N-methyltransferase inhibitor from macrocyclic peptide: Compound 14 (5)
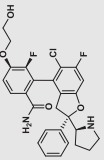
Nicotinamide *N*-methyltransferase (NNMT) is essential in the methylation of nicotinamide (NA) to 1-methyl nicotinamide. Since its discovery 70 years ago, NNMT has evolved from serving

Table 1 Overview on cases of transformation from peptides into small molecules.

Target	Peptide			Small molecule			Method	Ref.
	Name	Structure/Sequence	Activity	Name	Structure	Activity		
Nicotinamide *N*-methyltransferase (NNMT)	Macrocyclic peptide 1 (**1**)		NNMT inhibition: $IC_{50} = 0.10$ μmol/L	Compound 14 (**5**)		NNMT inhibition: $IC_{50} = 0.0011$ μmol/L	• HTS • X-ray • GIST • Ala scanning • Docking check	39
Viruses possessed 3CL proteases (3CLP)	–	EDLFYQ	3CL PPI inhibition: $IC_{50} > 300$ μmol/L	Compound 6j (**10**)		MERS-CoV 3CL PPI inhibition: $IC_{50} = 0.08 \pm 0.01$ μmol/L	• Pocket fitting design • Exploring key interaction pockets • Structure-based residue design	40 −45
Ghrelin receptor (GR)	Ghrelin peptide	GSSFLSPEHQRVQQRK ESKKPPAKLQPR	Ghrelin inhibition: $IC_{50} = 0.0031$ μmol/L	Compound 17 (**20**)		Ghrelin inhibition: $IC_{50} = 0.0003$ μmol/L	• Machine learning • Key structure identification • Score rating	46
Translocase MraY (TrM)	Motif of lysis protein E	Arg-Trp-x-x-Trp	Microbial inhibition: $MIC_{50} = 31$ μg/mL*	Compound 12b (**11**)		Microbial inhibition: $MIC_{50} = 4$ μmol/L[a]	• Natural environment analogue • Computational protein design • X-ray co-crystal	47, 48
Trypsin protein	–	ICPRIWMEC	ND	Compound 2l (**18**)		Trypsin displacing inhibition: $K_d = 2.1$ μmol/L	• EKO strategy • PPI overlay compare • Scaffold hopping	49
Spike protein of SARS-CoV-2 virus	Human ACE2 N-terminal helix	EDLFYQ	ND	Compound 7 (**6**)		Spike protein inhibition: $IC_{50} = 20 \pm 5$ μmol/L	• Pocket fitting design of the RBD interaction area • Dual-action design • Dipeptide substitution • PPI overlay compare	50
β-Herpesvirus proteases	Cyclic peptide 1 (**12**)		HCMV[Pro] inhibition: $IC_{50} = 0.0015$ μmol/L HHV6[Pro] inhibition: $IC_{50} < 0.076$ μmol/L MW: 1735	Compound 19 (**17**)		HCMV[Pro] inhibition: $IC_{50} = 2.5$ μmol/L HHV6[Pro] inhibition: $IC_{50} = 0.33$ μmol/L MW: 687 No. of HBD: 2	• mRNA display screening	51

(*continued on next page*)

Table 1 (continued)

Target	Peptide			Small molecule				Ref.
	Name	Structure/Sequence	Activity	Name	Structure	Activity	Method	
Transcriptional enhancer associate domain (TEAD)	Yes-associated protein (Ω-loop)	85–99 PMRLRKLPDSFFKPP	$K_d = 29 \pm 7$ nmol/L (wtYAP[61–99]) MW:18,300 No. of HBD: 21	IAG-933 (**26**)	*(chemical structure)*	YAP-TEAD inhibition in MSTO-211H cell line: $IC_{50} = 0.011$ µmol/L MW: 514	• High throughput *in silico* screening • GLIDE • Molecular modeling • Network analysis • AMBER • Free energy evaluation	52–56

[a]Against *E. Coli* 12. –Not applicable. ND, not detected.

only metabolic functions to being a driving force in various cancers critical to human health. Yoshida et al. reported a typical case of transferring a peptide into a small molecule in 2022[39]. They identified a novel NNMT small molecular inhibitor, compound 14 (**5**), modified from the macrocyclic peptide 1 (**1**, Fig. 1A)[57−59]. In this case, X-ray co-crystal structure analysis, pharmacophore analysis, *de novo* design and structure-based optimization contributed to the optimization of the lead compound (Fig. 1A).

Macrocyclic peptide 1 (**1**), a thioether-closed macrocyclic peptide, is identified by affinity selection-based peptide display technology and composed of eight residues (Phe1-F4CON2-Arg3-Gly4-HxG5-Trp6-Pro7-Cys8), including two non-natural amino acids: 4-carbamoyl-phenylalanine (F4CON) and *N*-hexyl-glycine (HxG)[60]. As shown in Fig. 1B, the X-ray co-crystal structure analysis indicated that macrocyclic peptide 1 (**1**) is located in a cave that contained a cryptic pocket (formation induced by the binding of macrocyclic peptide 1 (**1**)), a homocysteine pocket and a dimer interface. Arg3 and Gly4 were inserted into the homocysteine pocket, F4CON2 was located along the dimer interface, and Phe1, Pro7, Cys8, and Gly9 were exposed to the solvent. In addition, the binding of macrocyclic peptide 1 (**1**) induced a cryptic pocket to accommodate HxG5 and Trp6. Beyond recognition, to understand the pharmacophore of macrocyclic peptide 1 (**1**), a SAR study on this peptide was then conducted through alanine scanning and a hydration analysis based on grid inhomogeneous solvation theory (GIST) (Fig. 1C)[61−63]. The results of alanine scanning indicated that Arg3, Gly4, HxG5, and Trp6 strongly contributed to the binding activity. The GIST analysis and molecular dynamics simulation suggested that entropically unfavorable waters were clustered in the cryptic pocket, and the replacement of unstable water molecules by the two lipophilic side chains of HxG5 and Trp6 contributed to the strong binding upon the target[64,65]. Moreover, GIST indicated that the entropically unfavored water molecules frequently stayed around the carbonyl groups of Gly4 and HxG5 of macrocyclic peptide 1 (**1**), and the team speculated that these two hydrogen bond acceptors (HBAs) would act as anchoring interactions that displace the restrained entropically unfavored water molecules and form electrostatic interactions with NNMT. After the pattern discovery procedure, four main functional groups of macrocyclic peptide 1 (**1**) were finally defined as key pharmacophore queries for virtual screening: a homocysteine pocket that requires a positive charge, a hydrophobic cryptic pocket, and two HBAs interacting with the backbone NH of Tyr86 and Val143. Based on the results of binding mode and SAR analysis of macrocyclic peptide 1 (**1**), pharmacophore-guided *in silico* design of small molecule ligands was conducted (Fig. 1D)[66]. During a virtual screening using over six million fragments library, no compound satisfied all the features after filtering the obtained docking poses through pharmacophore queries. Then, they reduced the filter standard using three pharmacophore features in close proximity (two HBAs and hydrophobic features) and obtained fragment Virtual Hit-A. Starting from the Virtual Hit-A, *in silico* structural optimization by docking was performed. As shown in Fig. 1D, the structural extension toward the homocysteine pocket was performed first to obtain the designed molecule B, which satisfied the unused pharmacophore features left in the homocysteine pocket. The imidazolyl-methylene linker of the designed molecule B formed a polar interaction with the main chain carbonyl of Thr163, similar to macrocyclic peptide **1**. Thereafter, alternative substituents (preferentially occupied the cryptic pocket) on the nitrogen atom of the benzimidazole group were explored to obtain the designed
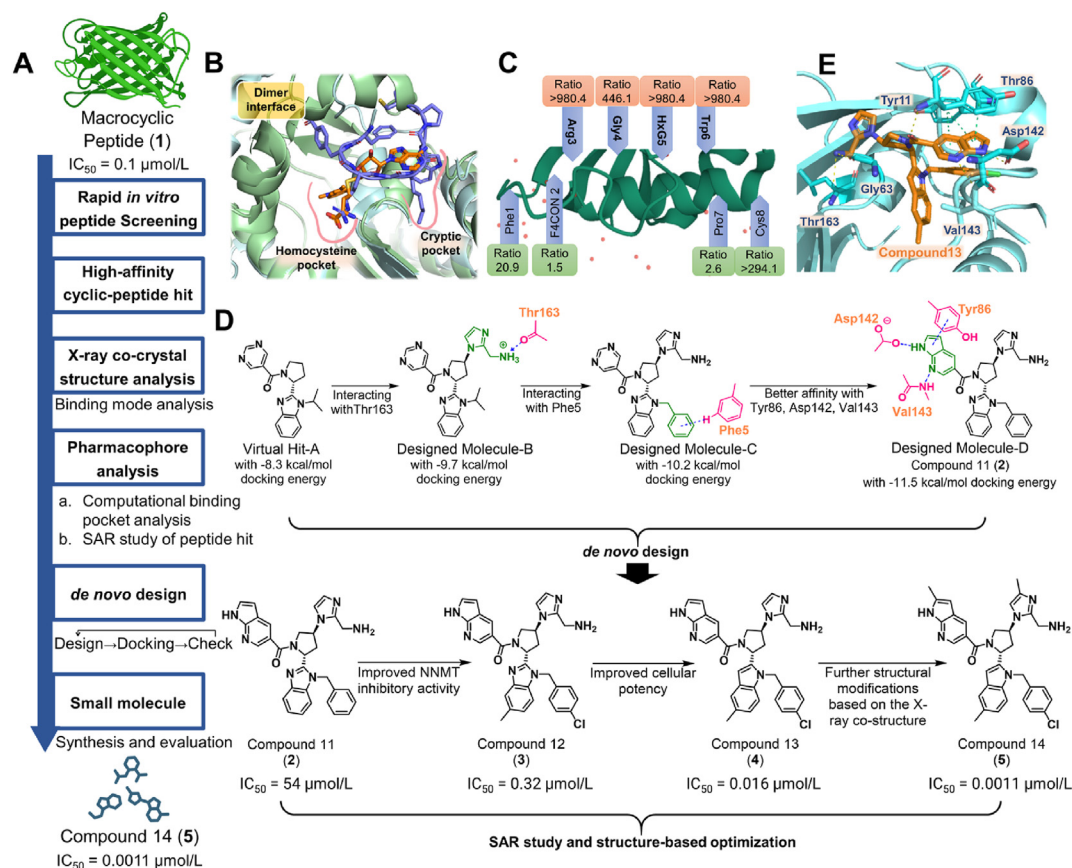
Figure 1 The discovery of Nicotinamide *N*-methyltransferase inhibitor (compound 14 (**5**)). (A) The overview workflow of the discovery of **5**. (B) The X-ray co-crystal structure analysis of compound 1 (**1**) in cave with cryptic pockets. (C) Structure—activity relationship study and alanine scanning result. The ratio measures the difference in activity between wild-type and alanine substitution. (D) The pharmacophore-guided *in silico* optimization from Virtual Hit-A to compound 11 (**2**), following by SAR study and structure-based optimization to obtain compound 14 (**5**). (E) The X-ray co-crystal binding structure and activity of compound 13 ($IC_{50} = 0.016$ μmol/L) (**4**).

molecule-C. The *N*-benzyl benzimidazole moiety of molecule-C could form a T-shaped $\pi-\pi$ interaction with the Phe5 side chain and Trp6 of peptide **1**. Finally, the pyrimidine moiety was replaced by an azaindole group that could form additional polar interactions with the side chain of Asp142 and parallel π-stacking with Tyr86 to obtain the designed molecule-D (compound 11 (**2**)). The *de novo*-designed compound 11 (**2**) was synthesized and exhibited weak but evident inhibitory activity against NNMT (Fig. 1D). The ^{15}N nuclear magnetic resonance (NMR) chemical shift perturbation experiments implied that compound 11 (**2**) specifically binds to NNMT in a manner similar to macrocyclic peptide 1 (**1**). A structure-based hit-to-lead optimization was first conducted based on the docking model of compound 11 (**2**), yielding compound 13 (**4**) with improved activity, as shown in Fig. 1E. Simultaneously, cocrystallization of the 13/NNMT complex was achieved, directing further structural modifications in small molecules. With the stepping-stone model of compound 13 (**4**), the following optimization based on SAR was swiftly conducted in cells and *in vitro*. Eventually, compound 14 (**5**) was obtained with the strongest cell-based activity and without cell toxicity (cell-based $IC_{50} = 0.40$ μmol/L, 50% cytotoxic concentration $CC_{50} > 10$ μmol/L).

In this case, Yoshida et al. successfully transformed the macrocyclic peptide 1 (**1**) into a small-molecule compound 14 (**5**)[39]. In second configuration, the research team proceed the *de*

novo design and optimized step-by-step using traditional approach of medicinal chemistry. Through peptide screening, cocrystal structure analysis, and shrinking side chains and residues, they successfully pulled out the superior candidate from the design-docking-check procedure. It is remarkable how technologies are being used to potential small molecules. It would be even better if a universal shortcut could accelerate the *de novo* design part, which is the most time-consuming part. Since this process is already well organized, the next hope is to move on to more rapid binding mode discovery and compound optimization. This method would be promising for peptides with a clear residue sequence, explicit cocrystal binding details, and moderate molecular mass below 20 amino acids.

2.2. Dual-action small-molecule inhibitors against COVID-19 3CLPro and RBD−ACE2 protein−protein interaction: Compound 7 (**6**)

The COVID-19 pandemic, caused by severe acute respiratory syndrome coronavirus 2 (SARS-CoV-2), resulted in over 612 million confirmed infection cases and 6.5 million associated deaths worldwide by September 2022[67−70]. Current clinical treatment often fails to relieve symptoms, leading to growing trends in finding complementary therapeutic approaches, such as inhibiting the major protease involved in the viral replication of

SARS-CoV[71−73]. The chymotrypsin-like cysteine protease (3CLPro), also known as M^{pro}, was selected owing to its high similarity among different types of coronaviruses, controlling the upstream regulation of the production of spike and membrane proteins, viral replication, and infection (Fig. 2A)[74−76]. The development of molecules targeting PPI is of interest to develop novel therapeutic agents[77−79]. Key events when invading human cells involve the virus using its receptor binding domain (RBD) protein to interact with human angiotensin-converting enzyme 2 (ACE2) to enter cells and complete the infection[80−82]. By inhibiting the 3CLPro function and impeding the PPI of viral RBD and human ACE2, a small molecule can have a dual action in advanced protection against the coronavirus. With this prospect, Tedesco et al. managed to design small molecules that have dual action on both 3CLPro and RBD-ACE2 PPI inhibition, inserting the ACE2 mimic sequence into the dipeptide isoform to inhibit the activity of SARS-CoV-2 3CLPro main protease, thus providing a way toward coronavirus infections[50]. Small molecules with dual-action design can inhibit the viral proteins necessary for their replication, such as the 3CLPro or the RNA-dependent RNA polymerase (RdRp), preventing the overlapping polyprotein pp1ab (∼750 kDa), which is crucial to viral replication and transcription[83,84]. Simultaneously, these small molecules can suppress viral PPIs, mostly mediated by an α-helical structure at the interacting surface. The evidence indicates the α-helix as a potential template[50,85].

Filomena's team started from the special ACE2 frame epitope to adapt a dual-action dipeptide and successfully pulled out the
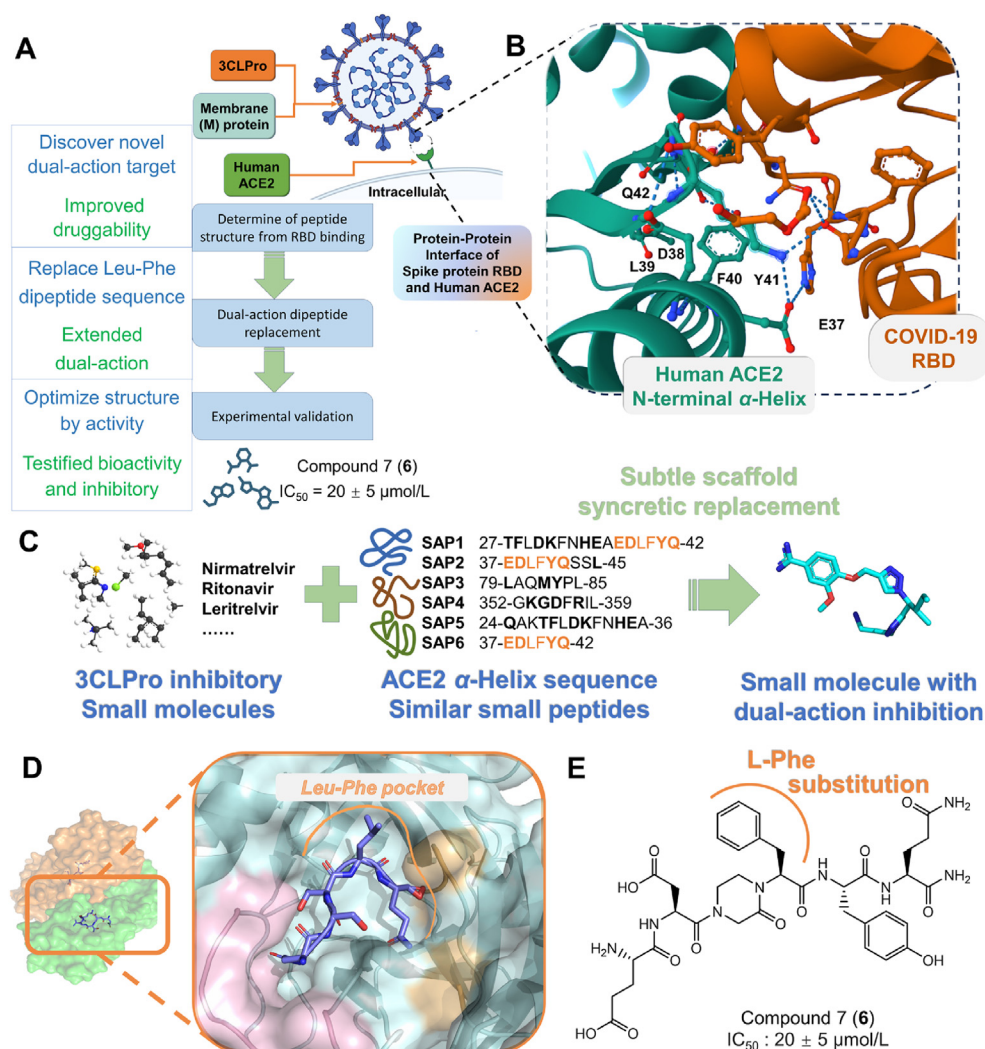

Figure 2 The small molecule design from viral spike protein. (A) The workflow of the research team of Trabocchi et al. from viral RBD region analyzation to dual-action small molecule compound 7 (**6**)[50]. The figure was generated from BioRender.com. (B) The binding details of human ACE2 N-terminal helix and viral SARS-CoV-2 Spike RBD. Main binding interactions exerts from Y505, N501, T500, Q498 and Y449. (C) By combining properties and structure of 3CLPro inhibitors and ACE2 α-helix mimetics, Trabocchi's team designed a dual-action small molecule[50]. 3CLPro inhibitors and Larue and Sharma's epitopes generated dual action inhibitors, the dual action compounds originating in the design of Trabocchi's group by matching the required glutamine flanking the cleavable peptide bond of 3CLPro substrate and the C-terminal glutamine found in epitopes as reported in the paper by Larue and Sharma[50,88]. (D) The Leu-Phe pocket region shows in ligand fitting mode, requiring especial dipeptide design to have better adhering activity (PDB ID: 1UK4). (E) The chemical structure of template peptide and the L-phenylalanine pocket.

candidate with bioactivity and inhibitory activity (Fig. 2B)[86]. Accordingly, several small-molecule inhibitors targeting the PPI of 3CLPro have been approved, including direct-acting antivirals such as Paxlovid containing nirmatrelvir (PF-07321332), molnupiravir, ensitrelvir, and remdesivir. Zhou et al. reported the fundamentals of the complex ACE2-S1 with SARS-CoV-2 spike protein[87]. This PPI is characterized by viral RBD interacting with the exposed domain of ACE2 with the N-terms of the α1 helix. Based on the interaction pattern, a frequently emerging epitope was identified for developing ACE2-spike protein S inhibitor based on particular interactions. From the analysis of initial work reported in the literature on identifying short epitopes of the ACE2 α1 helix, the team decided to design a peptidomimetic using the sequence H-37EDLFYQ42-NH2, starting from Glu37 to Gln42, as shown in Fig. 2C. Specifically, based on the sequence of ACE2 α1 helix, Larue and Sharma imitatively designed and tested a series of small peptides based on ACE2 to inhibit the spike−ACE2 interaction, revealing that the N-terminal epitope possesses the inhibition potency toward viral infection of SARS-CoV-2 down to the millimolar range (Fig. 2C)[88]. The team of Trabocchi especially chose the N-terminal epitope candidate that showed the most outstanding inhibition activity ($IC_{50} = 1.90 \pm 0.14$ mmol/L)[50]. To constrain this sequence and improve the druggability of the N-terminal epitope, the team replaced the Leu-Phe dipeptide sequence with dipeptide isosteres because the Leu-Phe residues are not directly associated with the spiral RBD. As shown in Fig. 2D, the purpose of this Leu-Phe sequence is to fill the special Leu-Phe pocket, as this sequence does not directly interact with the RBD of spike S1 domain, leaving the Leu-Phe pocket unfilled. Based on previous studies, Tedesco et al. used piperazinone to construct the main scaffold for the central dipeptide substitution, called "Leu-Phe substitution" (Fig. 2C)[89−91]. As the central backbone, the team evaluated the ability of these compounds to interfere with the ACE2-spike S1 RBD PPI via enzyme-linked immunosorbent assay[92−94]. After manually replacing functional groups around the Leu-Phe substitution, the team synthesized compound 7 (6) with an IC_{50} of 20 ± 5 μmol/L (Fig. 2E). Furthermore, this small-molecule inhibitor exerts dual-action activity in both spike-ACE2 PPI inhibition and 3CLPro reduction, with IC_{50} values of 15 ± 6 and 20 ± 5 μmol/L against 3CLPro and spike−ACE2 PPI, respectively. Compared with the previous millimolar activity, the enhanced performance may stem from refined structural analogies between the ACE2 N-terminal α1 helix and viral RBD epitopes, coupled with a dual-action design that more effectively recognizes and inhibits the M^{pro} motif. Filomena assumed that shared C-terminal Glu in the ACE2 epitope and 3CLPro binding site enables the creation of a dual-action structure[95,96]. The ongoing exploration aims to delve into finer detail and fundamental mechanics.

Larue and Sharma focused on short peptide inhibitors of spike−ACE2 PPI, whereas Trabocchi and collab. reported a dual-action compound based on the work of Larue and Sharma, and adding evidence about 3CLPro inhibition of their peptidomimetic compound to complete the delightful work of research to splendid compound 7 (6, $IC_{50} = 20 \pm 5$ μmol/L)[50,88]. This small molecule inhibitor contains a constrained dipeptide isostere, replacing the glycine-phenylalanine sequence in the peptide epitope EDLFYQ. The dipeptide isostere in turn, contains a 3-oxo-3,4-dihydropyrazine-1(2H)-carboxylate substituent at the C-terminus, which is a structural modification compared to the native glycine-phenylalanine sequence. In the study, compound 7 (6) showed inhibitory activity against the SARS-CoV-2 ACE2/

spike interaction in the micromolar range. Specifically, it was found to inhibit the interaction between the binding region domain (RBD) of SARS-CoV-2 spike protein S1 and ACE2 receptor. Furthermore, compound 7 (6) also exhibited inhibition of SARS-CoV-2 3CLPro main protease activity. The rationale behind this dual inhibitory property is the structural analogies between the N-terminal α1 helix of ACE2 and protease substrate epitopes, and in particular the concomitant presence of a C-terminal Q amino acid in both the key ACE2 epitope and the M^{pro} recognizing motif. Based on patient observation and residue replacement experiments, the study shows a new traditional approach. From the overall work of fantastic researchers, statistical data reveal no inhibition for the parent normal peptide epitope, suggesting the key role of the constrained dipeptide isostere in promoting the inhibition activity. This presents an additional path for enriching the drug candidate pool of COVID-19 in front of the repetitive riptides of the COVID epidemic caused by evolved variants.

2.3. Local molecule warhead component substitution for 3CLPro dimer interface: Compound 6j (10)

The category of small-molecule peptidomimetics, also known as "D-type peptidomimetics" in Grossman's classifications, employs a strategic approach for developing peptidomimetics based on focused modifications to reproduce the effectiveness of the original peptide[97]. Many viruses reproduce and replicate depending on the cleavage by catalyzation from dedicatedly encoded polyproteins with proteases, such as 3CLPro. The conservatory 3CLPro is a homodimer with a Cys145-His41 dyad, which catalyzes substrates such as pp1ab and provides an aperture extended for binding[98−100]. As shown in Fig. 3A, Chang et al. decided to invent novel small molecules against multiple coronaviruses, such as SARS-CoV-2, MERS-CoV, and picornaviruses, including picornavirus-like superclusters, such as caliciviruses (norovirus and sapovirus genera)[45,101,102]. As reported in a substrate specificity analysis, 3CLPro exhibits a strong preference for a -haa-N-Leu-Gln-aa sequence (haa = hydrophobic amino acid, aa = small amino acid, N = diverse residues exposed to solvents, such as Val, Lys, and Thr)[103]. Chang et al. decided to inhibit 3CLPro dimer formation to inhibit the protease activity and obtain viral suppression[104]. After the affinity sequence identification, pocket-fitting design, and property modification, they successfully discovered small-molecule inhibitors with an aldehyde, compound 6j (10), as examples (Fig. 3D).

The design of GC-376 (8) was inspired by replacing the amide bond and other local variations to mimic key protein structures such as β-turn and β-sheets[38]. A recent overall analysis of peptidomimetics in the market or under clinical trials showed that GC-376 (8) has versatile applications beyond feline peritonitis virus. Identification of the target 3CLPro peptide for GC-376 (8) involved investigating the side chain conformations and functionality requirements through current methods, such as single amino acid modification or replacement[105,106]. Three commonly used methods for identifying the essential site in 3CLPro are truncation studies, alanine scan, and N-methylation[107,108]. The truncation study is the most defining procedure for identifying the minimal sequence with peptide bioactivity[109,110]. Finding the best small molecule transformed from a peptide is likely achieved by replacing molecular groups for amide bonds and other local variations. One of the most common strategies involves substituting the native nitrogen atom in the amide backbone with oxygen to produce an ester, with the advantage of reducing peptide features,
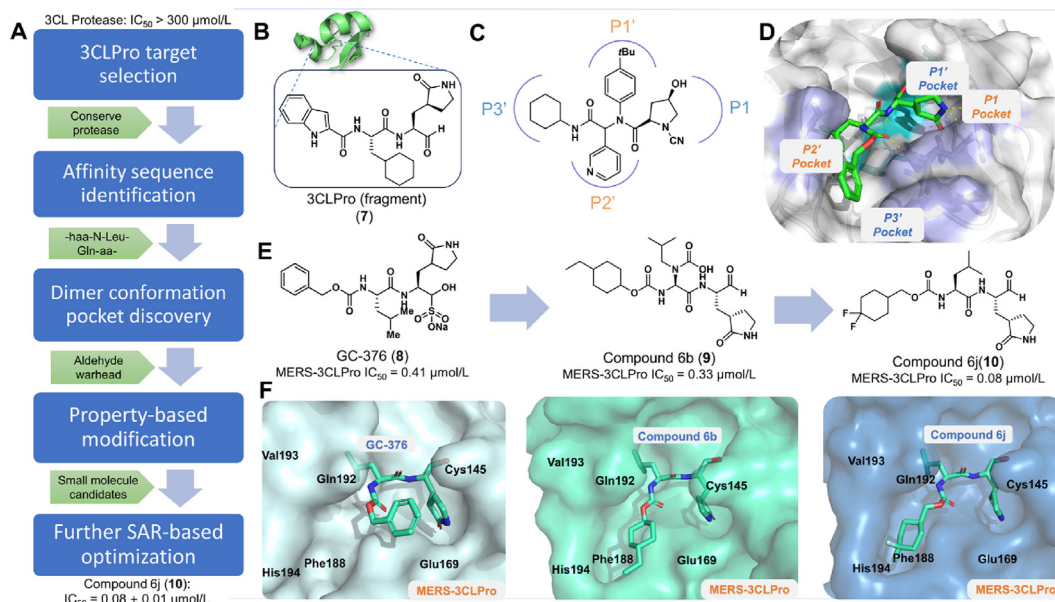
Figure 3   Discovery workflow of anti-viral small molecule compound 6j (**10**). (A) The chart of procedure from potential peptide structures into small molecule with modification and simulation. (B) Structure of 3CLPro fragment, sketch for the core mimic designing site. (C) Schematic scaffold in binding site, into four key feature pockets in P1, P1′, P2′ and P3′ giving clues to potential compound candidates. (D) The binding pattern of GC-376 (**8**) with main protease of SARS-CoV-2. (E) Structure and activity of GC-376 (**8**), compound 6b (**9**) and compound 6j (**10**). (F) The binding details of GC-376 (**8**), compound 6b (**9**) and compound 6j (**10**) with MERS-CoV 3CLPro.

improving metabolic stability, and contributing to a diverse secondary structure assembly of peptidomimetics[111−113]. As studied by medicinal chemists, different types of antiviral peptidomimetics have been applied to cure coronavirus and other infectious diseases, targeting a wide spectrum with various structures, including α-acyloxymethylketone, aldehyde warhead, α-ketoamide[41,114]. This instills growing confidence in researchers globally to introduce small molecules against viruses. Several research teams initiated work from proteins in the cysteine protease family mediating the viral replication and transcription by cleaving the polypeptide into structural and nonstructural proteins. The Cys45/His41 residues enclosed in the S1/S2 pockets, as shown in Fig. 3C, are important to the binding process. Citarella et al. discovered this type of peptidomimetic inhibitor of the main protease (M^{Pro}) of SARS-CoV-2, exactly referencing the same pockets and residues with the catalytic dyad, including Cys45/His41[115,116]. The enzyme mainly hydrolyzes the bonds between P1 glutamine and P1′ amino acids, such as alanine and glycine (Fig. 3D)[117]. The series compounds designed under the guidance of four pockets of propensity exhibited the inhibition potential against MERS-CoV-2 (IC$_{50}$ = 0.08 μmol/L).

Currently, other candidate inhibitors, such as compounds 6b (**9**) and 6j (**10**), shown in Fig. 3E, are in the laboratory development procedure. The binding of GC-376 (**8**) to the 3CLPro pocket was not sufficiently settled, leaving a certain free space between Gln192 and Cys145. Thus, an aldehyde warhead was used to introduce additional hydrogen bonds to the surface of pockets. Further inspection of crystal structures shown in Fig. 3F revealed that the inhibitors that bound to MERS-CoV 3CLpro have the potential to achieve enhanced binding interactions within the S4 pocket with appropriately decorated cyclohexane derivatives while eliminating sulfonate in GC-376 (**8**) structure. While maintaining the major structure of GC-376 (**8**), the team designed and synthesized a series of compounds. Among them, compound

6b (**9**) introduced the aldehyde design, and compound 6j (**10**) presented the best inhibitory activity. During the reaction, the aldehyde targets 3CL protease and binds to the active site of 3CL protease, casting its sulfite group structure to expose the aldehyde, which reacts with the nucleophilic cysteine residue of 3CLpro to form a reversible covalent bond[44]. The warhead design obstructs the catalytic action of 3CL-like protease, thus inhibiting viral replication, resulting in outstanding inhibitory activity (IC$_{50}$ = 0.08 ± 0.01 μmol/L)[42−45]. By far, there are additional AMK small molecular inhibitors, including GC-376 (**8**), under laboratory biological development.

Despite the promising applications of small molecules modified from peptides drawing interest from research teams worldwide, considering the larger spatial requirements and interaction conformations of macrocyclic peptides, small molecules still fall short in compensating for all restrictive conditions at once[118,119]. Combining properties from molecules and peptides may simultaneously obtain disadvantages from both. In the more practical application of drug development, small molecules are more favorable in efficiency than actual peptides that bind to protein bonds. This study introduced a solid base of classical workflow of sequence identifying-binding pockets discovery-SAR optimization, in the transformation from peptides into small molecules. Furthermore, a set of "toolbox" molecules can quickly determine properties of peptides by simulating interaction, fulfilling structure, or holding tight to key scaffolds, especially in the high-throughput era driven by machines and AI.

2.4.   Antimicrobial peptidomimetics targeting translocase MraY and bacteriophage φX174 protein−protein interface: Compound 12b (**11**)

In 2021, Kerr et al. reported a case of peptidomimetic analogs of an Arg-Trp-x-x-Trp motif responsible for inhibiting the interaction
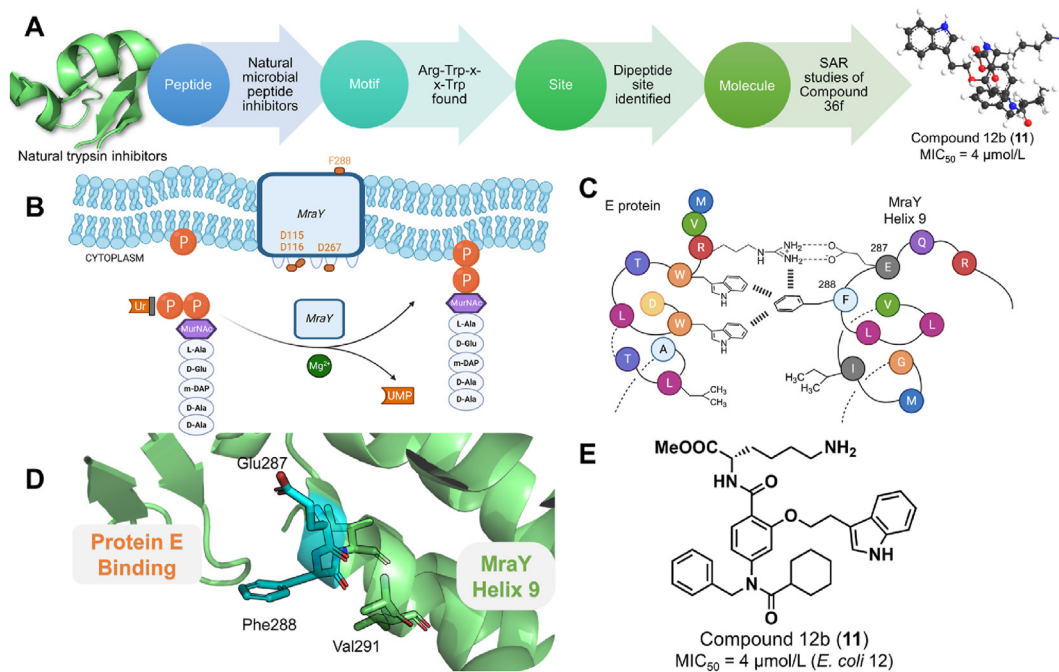
Figure 4 The discovery of microbial translocase MraY interface inhibitor: compound 12b (**11**). (A) The discovery procedure of translocase MraY inhibitor from potential peptide structures into small molecules. (B) Examples of reactions catalyzed by MraY, including constructing the lipid membrane. The figure was generated from BioRender.com. (C) Given by Kerr and research team, the model for interaction site between N-terminal part of protein E and helix 9 of MraY[47]. The figure was generated from BioRender.com. (D) The key binding site Phe288, and of important structure Phe286/Glu285 in Arg-Trp-x-x-Trp motif. (E) Structure of compound 12b (**11**), exhibiting the most outstanding inhibitory activity against *E. coli* K12 (IC$_{50}$ = 4 μmol/L).

of phospho-MurNAc-pentapeptide translocase (MraY) with bacteriophage X174 lysis protein E (Fig. 4A)[47]. Simultaneously, MraY is the target for mureidomycin/pacidamycin uridyl peptide antibiotics, liposidomycin liponucleosides, and muraymycins. If researchers can simulate the translocase MraY, it can obstruct the catalyzation of lipid intermediate I during bacterial peptidoglycan biosynthesis, leading to the death of microorganisms[120,121].

The translocase MraY catalyzes the formation of lipid intermediate I in bacterial peptidoglycan biosynthesis and was found to be the target of bacteriophage lysis protein E (Fig. 4B). However, the well-known catalyzation site is far from the interaction site between MarY and lysis protein E[122]. The interface between them is mediated by Phe[288] and Glu[287], with the necessary Phe[288] located on the extracellular face on helix 9 of MraY (Fig. 4C). The other component, φX174 lysis protein E, is a 91-amino acid protein with transmembrane and soluble domains on both its N-terminal and C-terminal. A 37-amino acid synthetic peptide referred to as Epep was found able to inhibit particulate *E. coli* MraY at IC$_{50}$ = 0.8 μmol/L; nevertheless, this activity was no longer maintained with detergent-solubilized MraY, indicating the remoteness of PPI and active site[123]. Besides *E. coli* MraY, an Arg-Trp-x-x-Trp motif was found on protein E in several cationic antimicrobial peptides. In 2014, Rodolis et al. demonstrated the antibacterial activity of the dipeptide Arg-Trp octyl ester and concluded that the dipeptide fragment functioned as a mimic toward the target of MraY[48]. Kerr and the research team quickly analyzed the active site of lysis protein E and found that the possible binding sites were Arg[3], Trp[4], and Trp[7], forming interaction aromatic bonds with MraY Phe[288]; Proven in another research, the Arg-Trp-x-x-Trp motif appears to have inhibitory

activity against *E. coli* MraY (IC$_{50}$ = 200−600 μmol/L)[48]. Thus, the research team identified the Arg-Trp-x-x-Trp motif as the main template to mimic, which binds to the Phe288 and Glu287 at the Helix 9 binding site (Fig. 4D). A previous study synthesized a 37-amino peptide containing the N-terminal transmembrane domain to inhibit particulate *E. coli* MraY (IC$_{50}$ = 0.8 μmol/L). Nevertheless, no activity was detected after the MraY was detergent-solubilized, suggesting that protein E inhibits a PPI area remote from the MraY active site. Although barely any inhibition activity was observed when imitating the Arg-Trp-x-x-Trp sequence by synthesizing pentapeptides, the dipeptide analog of Arg-Trp-octyl ester excelled over other candidates with MIC$_{50}$ values of 31 and 8 μg/mL against *E. coli* K12 and *Bacillus subtilis*, respectively. At a closer look, the interaction site between MraY and lysis protein E appears to be remote from the enzyme active site; the complete Arg-Trp-x-x-Trp mimicking pentapeptides exhibited no antimicrobial activity, but the activity of the dipeptide analog Arg-Trp-octyl ester was observed. With this observation, they pulled out groups of candidates from Arg-Trp-oct, Arg-Trp-x-x-Trp, and the original peptide. The research team studied several previous cases that target PPIs, such as MDM2−p53 and Bcl-XL/Bak, to discover better solutions to mimic the residue structures[124−126]. Inspired by previous research about simulating aromatic ring systems in amino acids, Kerr and the team synthesized the first series of compounds[47]. However, their activity was not considerably improved compared to the original dipeptide Arg-Trp. The team suspected that the C-4 of the benzene was not properly functioning, so two new series of monoalkylated and dialkylated peptidomimetics were designed to use C-4-modified benzene to mimic the Trp residue in the final edge of the Arg-Trp-x-x-Trp

motif. This new series of compounds showed promising antimicrobial activity. Peptidomimetics 12b (**11**) and the series compounds had MIC_{50} values of 4−8 μg/mL against *E. coli*, indicating this scaffold is an appealing chemotype for further optimization (Fig. 4E).

In the hope of finding more potential targets on the exterior face of the cytoplasmic membrane, Kerr et al. conducted SAR studies on Arg-Trp-oct for antimicrobial action. Since the target is involved with the binding site of α-helix protein E, the team leveraged advantages from precedent cases[47]. A deep SAR study of this motif was conducted to determine the best structure of novel α-helical peptidomimetics. Candidates from compound 12a to compound 12g were reported with much better inhibitory concentration against *E. coli* K12, etc. Among them, compound 12b (**11**) stood out with promising activity, validating the translocase MraY as a druggable target and providing a novel small molecular scaffold for peptide mimicking. However, in this case, the design and optimization of atom sites correspond to the specific aromatic structure of the small molecule design. Additional examples focusing on different types of amino acids can enrich peptide reforming strategies in highly universal situations.

2.5. Peptide-to-small molecule design of active-site β-herpesvirus proteases inhibitors: Compound 19 (**17**)

Viral proteases play a crucial role as regulators in viral replication and assembly, making them promising targets for antiviral drugs. Proteases have been demonstrated as effective agents against human immunodeficiency virus and hepatitis C virus, providing a potential solution for organ transplant recipients or individuals with compromised immune function[127]. Human cytomegalovirus protease ($HCMV^{Pro}$) possesses a noncanonical catalytic triad consisting of nucleophilic Ser132 and histidine residues His63 and His157, forming a homodimer upon activation[128−130]. Protease inhibitors that bind to the active site are particularly attractive, as resistance mutations could potentially be lethal. Yoshida et al. reported another case where peptides were converted into small molecules, extending the success of the "peptide-to-small molecule" strategy and overcoming limitations associated with cyclic bulky peptide inhibitors[51]. With the assistance of computational methods, the team started the process with a rapid mRNA display screening, facilitating *de novo* design based on structural information from high-affinity macrocyclic peptide ligands (Fig. 5A).

First, to identify structural information on high-affinity cyclic peptide ligands, Yoshida and his team conducted a rapid mRNA display screening. The exploration of large chemical libraries, comprising up to 10^{12} diverse peptides, was realized through methods like the flexible *in vitro* translation system and transcription-translation coupled with the association of puromycin linker display, contributing to the development of peptide display methods[51,131−135]. Cyclic peptide 1 (**12**) emerged as a hit peptide during this screening that exhibited excellent activity ($IC_{50} = 0.0015$ μmol/L) despite its thioether-linked macrocyclic peptide weighing over 1700 as a 14-mer. Subsequently, peptide 1 (**12**) was successfully cocrystallized with $HCMV^{Pro}$, indicating a chimera protein pocket with transplanted assignable residues 135−137 from $HCMV^{Pro}$. Using SiteMap analysis and the hydration analysis based on grid inhomogeneous solvation theory (GIST), side chains of His5, Tyr6, and Trp7 were confirmed to form hydrophobic pockets. As shown in Fig. 5B, the residues Ile2-Trp7 were observed to form interactions from peptide 1 (**12**) to $HCMV^{Pro}$, indicating that this side chain may contribute to the displacement of energetically unfavorable water molecules to enhance the affinity of peptide 1 (**12**) and $HCMV^{Pro65}$. A SAR analysis was then conducted to evaluate the essential residues. As depicted in Fig. 5C, alanine-scanning mutagenesis illustrated the importance of Ile2, Tyr6, and Trp7, as their mutation led to over a 100-fold decrease in activity. In addition, substantial reductions were observed for Thr3 and His5, suggesting their important role in stabilizing the conformation through intramolecular hydrogen bonds rather than simply filling the pocket, as shown in Fig. 5D. SAR studies by Ogilvie et al. further supported that the peptide 1 (**12**) backbone of chain NH and carbonyl of Ile2 formed a complementary pair of polar interactions with the backbone amide of Ser135, and carbonyls of Thr3 and His5 obtained helpful polar interactions with Arg165[136]. This observation defined three hydrophobic features (residues of Ile2, Tyr6, and Trp7), three HBAs (polar contacts with Ser135 and Arg165, and a positively charged side chain of Arg165), and a hydrogen bond donor (Ser135), as the key pharmacophore queries for *in silico* small-molecule design. The next step involved defining the secondary structure that mimics the bent main chain structure of Gly4 of the cyclic peptide (**12**). To find a cyclized skeleton, imidazolidinones were selected by the researchers because of their varied experiences in antiviral reagents and their ability to introduce various substituents through chemical modifications[137]. The authors selected the 4-carboxyamide-substituted imidazolidinone scaffold to achieve structural elongation to the pharmacophore queries while acquiring key interactions between Thr3-Gly4 and the protein. Fig. 5D illustrates the 3-amino-2-hydroxypyridine derivative, transition molecule (**13**), which mimics the key pharmacophore features of Ile2 through virtual screening of carboxyamide derivatives. At this site, the researchers considered substituents should satisfy forming polar interactions with the side chain of Arg165, as in peptide 1 (**12**), and fill the protein pocket similar to the side chain of His5 (Fig. 5E)[51]. The molecule **13** placed the terminal lipophilic group *via* a 5-membered heterocyclic linker from the benzyl position, filling the hydrophobic pocket as if it were the side chain of Trp7 in peptide 1 (**12**). To further occupy the phenyl pyrazole pocket, intermediate molecules (**14**) and (**15**) were generated and picked by the virtual screening algorithm to enhance docking energy and binding activity (Fig. 5D). For the final step, the authors conducted a SAR study of herpesvirus protease candidate molecules to refine the inhibitory activity. As shown in Fig. 5D, Yoshida et al. demonstrated a *de novo* pocket-fitting design to improve $HCMV^{Pro}$ inhibitory activity[51]. The 2-hydroxypyridine structures in molecule 13 (**15**) were replaced by the bicyclic lactam of molecule 14 (**16**) to fit into the bicyclic lactam pocket[51]. The ortho position of the phenyl ring was substituted with pyrazole to fill the gap between $HCMV^{Pro}$ and the peptidomimetic ligand (Fig. 5E). From 32% inhibition at 99 μmol/L of molecule 13 (**15**), the partial pocket-fitted molecule 14 (**16**) exhibited an IC_{50} of 9.8 μmol/L, while the sufficiently occupying molecule 15 (**17**) demonstrated a favorable IC_{50} of 2.5 μmol/L against $HCMV^{Pro}$. In retrospect, as shown in Fig. 5F, the original peptide, shown in red surfaces, has been greatly streamlined into the small-molecule 15 (**17**), depicted in orange sticks, while maintaining an acceptable activity level. The authors have successfully demonstrated the feasibility of using this peptide-to-small molecule strategy to optimize the drug-like properties of peptides and convert them into small molecules with improved potency, selectivity, and pharmacokinetic profiles.
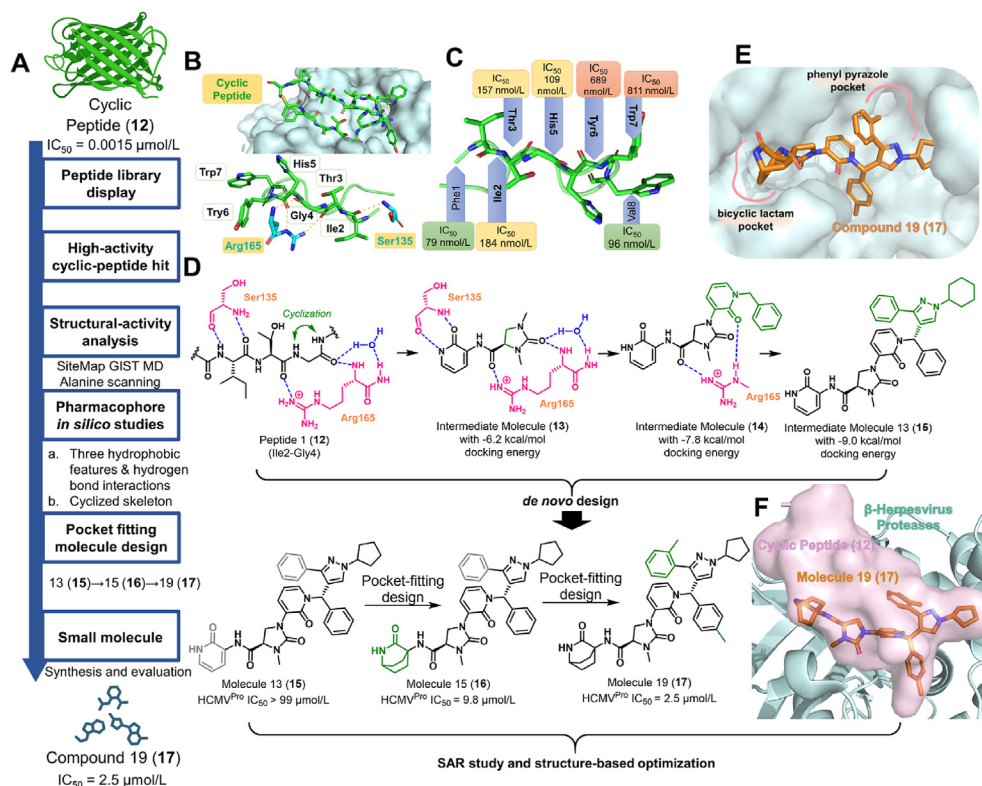
Figure 5 The discovery of non-covalent, active-site small molecule β-herpesvirus inhibitor (compound 19 (**17**)). (A) The overview workflow of the discovery of compound 19 (**17**). (B) The X-ray co-crystal structure analysis of cyclic peptide (**12**) binding with HCMV[Pro], and interactions of peptide Ile2-Trp7 with HCMV[Pro] residues. (C) Alanine scanning result of cyclic peptide amino acids, cell-free IC_{50} of HCMV[Pro]. The color represents differences from native peptide and mutation type, from red to yellow and green indicates the importance of each residue. (D) The pharmacophore-guided *in silico* optimization from cyclic peptide 1 (**12**) to intermediate molecules (**13–15**) and active molecules (**15–17**). The SAR study and structure-based optimization was performed to obtain compound 19 (**17**). (E) The binding pattern and two pockets to be fitted by compound 19 (**17**). (F) The simplification from cyclic peptide (represented in red) to small molecule (**17**, represented in orange) when binding the β-herpesvirus protease (HCMV[Pro], represented in pale blue).

As the authors expected, the "peptide-to-small molecule" approach, which involves the custom design of small molecules based on the pharmacophore characteristics of high-affinity peptides, is an excellent supplement to other hit-finding strategies for small-molecule drug discovery. These strategies include traditional high-throughput screening (HTS), fragment-based screening, and DNA-encoded library screening. This method offers a unique perspective, providing a tailored solution in drug discovery. This approach can potentially expand the scope of drug targets beyond traditional small molecules and biologics, enabling the discovery of new classes of therapeutics for viral diseases and other indications. The utilization of co-structure analysis, alanine scanning, GIST molecular dynamics analysis, pocket fitting, and SAR optimization has now become a systematical workflow that fuses classical methods and novel technologies for transitioning from peptides to small molecules. The two cyclic peptide cases and other remarkable achievements by Yoshida and the team are expected to expand the applicability of cyclic peptides[39,51]. Further optimization of the inhibitors and evaluation of their efficacy and safety in preclinical and clinical studies will be necessary to advance them toward clinical use. In addition, the "peptide-to-small molecule" strategy can be applied to other drug targets and disease areas, potentially leading to the discovery of new drugs with improved efficacy and safety profiles. Overall, this study provides a valuable contribution to the field of drug discovery and highlights the potential of innovative strategies to address unmet medical needs.

3. Computational intelligence aided transformation from peptide to small molecule

3.1. Small-molecule trypsin inhibitor from peptide through EKO strategy: Compound 2l (18)

In 2022, Lyu et al. obtained a novel small-molecule compound 2l (**18**), optimized from natural trypsin inhibitors, based on the structure of a series of natural peptides (Fig. 6A)[138–143]. The whole process was guided by a recent analysis method, "EKO strategy." Briefly shown in Fig. 6B, this strategy, proposed by Lyu et al., begins with identifying the interface of interest to residues[49]. It then uses a chamber and database to obtain structurally characterized ligands, ultimately overlaying the best-matched small molecule[144]. The EKO strategy, introduced by Perez et al., represents one of the earliest data mining approaches to match PPIs with probes *via* virtual affinity selection from a vast PPI library using specific small-molecule baits[145].

Lyu et al. discovered a common segment, called the "interface triplet," among six naturally occurring trypsin inhibitor proteins. This discovery was made by analyzing a similar structure
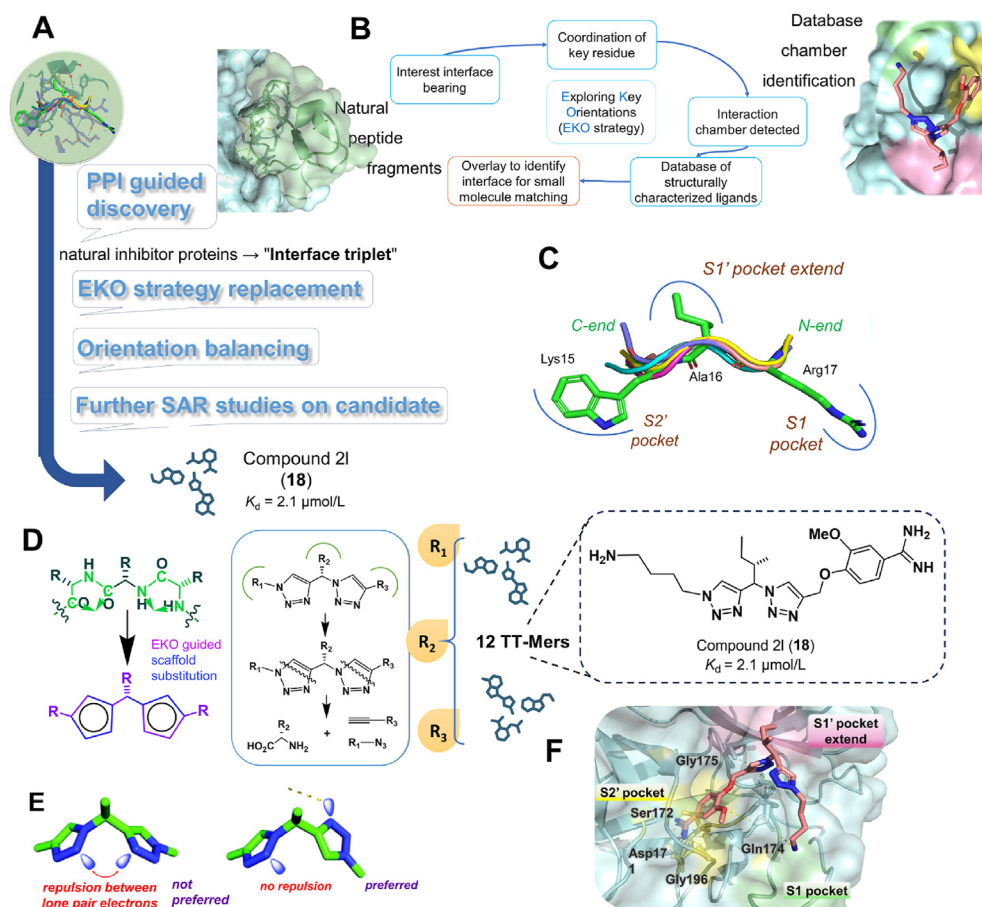
Figure 6 The design of ghrelin inhibitor compound 2l from peptides by EKO strategy. (A) The workflow of this case from trypsin inhibitor peptides and interfaces into small molecules. (B) The basic procedure of Exploring Key Orientation (EKO) strategy. (C) The overlay structure of trypsin inhibitor aligned with six natural trypsin inhibitor ligands, indicating three pockets: S1, S1′, S2′ (Burgundy red: Infestin-1, PDB 2F3C; pale pink: Bowman-Birk type trypsin inhibitor, PDB 3RU4; yellow: Buckwheat trypsin inhibitor, PDB 3RDZ; mint: Kunitz-type trypsin inhibitor, PDB 1ZRO; blue: ecotin, PDB 4NIY; pink: *Enterolobium contortisiliquum* trypsin inhibitor, PDB 4J2Y). (D) Replacement of peptide backbone to 5-membered aromatic rings when filling triplet regions, the EKO strategy gave the scaffold alignment to bovine pancreatic trypsin inhibitor (PDB: BPTI) with RMSD of 0.37 Å. Retro-synthesis analysis of 5-membered aromatic triazoles as replacement of the peptide backbone giving out 12 TT-Mers. Among 12 TT-Mers, chemical structure compound 2l (**18**) stands out with better K_d activity. Figure was generated from BioRender.com. (E) Conformation twist made by lone pair electrons of two triazole rings that may apply *cis*- and *trans*- orientations. (F) The interactions appeared between molecules and three pockets, salt bridge and hydrogen bonds. The detail of co-structure of compound 2l (**18**) and trypsin protein, three pockets of triazoles are also indicated in pale green (S1 pocket), light yellow (S2′ pocket) and light red (S1′ pocket extend).

fingerprint, consisting of three residues and occupying three pocket extensions (S1, S1′, and S2′, Fig. 6C) in the active site of trypsin[49]. This segment appears to dominate the interaction energy in PPIs. Subsequently, the team conducted a peptidomimetic design based on the key features of the interface triplet and evaluated them using the EKO strategy. As shown in Fig. 6D, the team used two five-membered ring motifs to replace four consecutive peptide backbone atoms, with the fifth atom stabilizing a certain conformation using tension from the ring[113]. The EKO strategy was then deployed to evaluate the best scaffold for inhibitory binding small molecules. Among all the tripeptide mimics scanned, one kind, consisting of two triazoles and colloquially referred to as the "TT-Mer" molecules, emerged as a promising simulator solution. Fig. 6D illustrates its alignment with the interface triplet, evidenced by an RMSD of 0.37 Å and apparent ease of synthesis[49]. Next, the team designed and

synthesized 12 "TT-Mer" variant molecules (compounds 2i−2l) with different substitute groups R_1, R_2, and R_3 (Fig. 6D). Among these 12 compounds, compound 2l (**18**) exhibited the strongest binding affinity with a dissociation constant (K_d) value of 2.1 μmol/L. As shown in Fig. 6F, the crystal structure of compound 2l with trypsin was solved, indicating three pockets with orientations of three potential substituent groups. Side chains R_2 and R_3 occupied the S1′ and S1 pockets corresponding to the interface triplet in the parent PPI used for the EKO analysis. Benzamidine group on the R_3 substituent formed a salt bridge with Asp189, as well as hydrogen bonds with Ser190 and the backbone carbonyl of Gly219. This strategy proposed key speculation that conformations overlay well and can be reinforced in the protein receptor when R_1−R_3 substituent groups in Fig. 6D correspond to appropriate regions of the protein−ligand interface. Following the small-molecule mimicry, candidates like compound 2l, with high

affinity (K_d = 2.1 µmol/L), can be subjected to further pharmacophore-guided design and additional SAR studies to take full advantage of them.

In a general sense, the adaption of the EKO strategy illuminates a new path for designing small-molecule peptidomimetics. This approach is valuable for quickly identifying position of interests and finding the best scaffold and function groups. It establishes a universal path for modifying small molecules from peptides for target proteins, with low cost, a much-reduced cycle, and the potential for broad application. Nevertheless, some topics remain to be discussed. When deciding the favorable conformation, the force field used for molecular mechanics in EKO was assisted model building and energy refinement (AMBER). However, it may suffer from a deficiency of energy gap resolution below the cutoff threshold from EKO analysis (3 kcal/mol)[146,147]. Consequently, both conformation forms were classified as "populated" in the EKO strategy because of their similar differences. There should be additional validation tools for the EKO strategy and small-molecule candidates in the future. Typically, when facing the protein interface, finding natural high-affinity ligands towards desired receptors could be a great option. Highlighted with the EKO strategy, the team overlayed peptides with mass molecular weight to find key structures rapidly and conveniently. However, aspects of the EKO strategy can still be improved. As shown in Fig. 6E, the conformational twists are too subtle to be detected within the detection limit using EKO measures. One additional experimental validation step would be needed nonetheless. In any case, this novel strategy is a splendid option form a high-affinity natural peptide library to create small molecules.

3.2. Novel tech-aided peptidomimetic design: Ghrelin receptor inhibitor compound 17 (20)

The field of AI-aided drug design has been broadly developed for decades. ML, a technology within AI, enables computer systems to learn from data and improve performance without explicit programming[148−151]. In simple terms, ML allows machines to automatically discover patterns and rules from large amounts of data, empowering them to make predictions or decisions[148]. Inspired by previous research reported by David Baker and his team, who used reinforcement ML to sample and design peptides, Liu et al. introduced a process for transforming peptides into small molecules using powerful ML. This reveals a new workflow for modifying proteins and peptides (Fig. 7A)[46,152]. Researchers are now attempting to apply ML to inhibitor design targeting ghrelin receptors (GRs). GR, also known as the growth hormone secretagogue receptor, comprises 28 amino acids and plays a crucial role in growth hormone metabolism and glucose homeostasis (shown in green, Fig. 7B)[153−155]. Positron emission tomography (PET) is the imaging technology in clinical approach for diagnosis and prognosis based on molecular interactions to validate drug leads in vivo prior to clinical trials[156,157]. In drug discovery, PET functions as medical imaging technique that is used to visualize the metabolic processes and functions of tissue using radioactive tracers, to validate the evidence in structure and activity relationships[158]. However, in current research, peptide substrates were also found effective in targeting GRs but quickly degraded in the gastrointestinal tract[159−162]. To overcome this drawback using a practical ML model, the key features of peptides must be determined and then computational intelligence can be applied in the design process.

In this case, the team chose ML to guide the transformation of peptides and peptidomimetics from huge database into small molecules. After balancing three modeling strategies and optimizing the best method of input ingredients, compound 17 (20) was selected as part of the external dataset used to evaluate the applicability of the machine learning model in real-world situations, demonstrating outstanding activity (IC_{50} = 0.3 nmol/L). Liu et al. first extracted all molecules with binding affinity to GR from the ChEMBL library, forming a potential first database of 1444 molecules recorded with binding activity. From this database, 1080 binding compounds with outstanding µmol/L-level binding were selected as the "binding" database[46]. To avoid biased prediction, Liu et al. selected 1297 random molecules from the ChEMBL library, with molecular weights between 320 and 2000, as the "random" database[46]. The team trained various ML models using a training dataset that exclusively contained peptides or small molecules or a combination of both. This approach was employed to assess whether ML models trained with distinct datasets (peptides only, small molecules only, and a mixture of both) could effectively predict small molecule binders[163,164]. Then, Liu et al. established an ML model to guide molecule design, retrieving binding data from the ChEMBL database, gathering key molecule fingerprints, and generating different ML models from various splitting plans, incorporating different datasets of small molecules and small peptides[165]. As shown in Fig. 7B, possible candidates with common structures, such as benzothiazole and large rings formed via peptide bonds, were clustered into groups. Three possible algorithms, random forest, support vector machine (SVM), and extreme gradient enhancement, were used to construct ML models (Fig. 7C)[166,167]. All test data groups with peptides/peptidomimetics into small-molecule arrays exhibited extraordinary prediction abilities. After processing with algorithms, the team looked for the best structure for molecules, obtaining useful information with versatile algorithms and by characterizing drug molecules based on molecular descriptors[168]. Before determining key features, researchers looking to set up a solid basis for molecules need a rigid and reliable scaffold. For molecular representations, as shown in Fig. 7B, the team used the Morgan fingerprint (MF)[169,170]. This popular circular topological descriptor encodes fragments for a structure with a 1024-bit hashing function based on its circumstances, representing sufficient data of the key interacting site. SHapley Additive exPlanations (SHAP) scores, developed from a game theory approach, are representations of feature importance calculated to explain the output of ML models[171,172]. The team treated the ROC scores, accuracy, f1, and MCC scores as the foundation for ranking different models. To understand GR interactions, key features from MF were selected, including conjugated ring systems, amine groups, and oxygen-containing groups actively involved in ligand-receptor interactions with GR[173]. Conversely, aliphatic and aromatic carbons provide hydrophobic environments that attract nonpolar parts of GR, resulting in a stronger global binding than training sets[174]. After a SHAP analysis, the final structure was determined through the overall design of three algorithms (Fig. 7D). In the final validation, the research team used a series of small-molecule fluorine-bearing quinazolinone GR antagonists recently discovered with high binding affinity as external data to confirm the ML result. Surprisingly, a structure similar to compound 21 was discovered by another research team in 2020 (IC_{50} = 15 nmol/L). Based on the data in the library presented by MF, as shown in Fig. 7E, compounds 21 (19) and 17 (20) exhibit similar structures; the only difference is they were
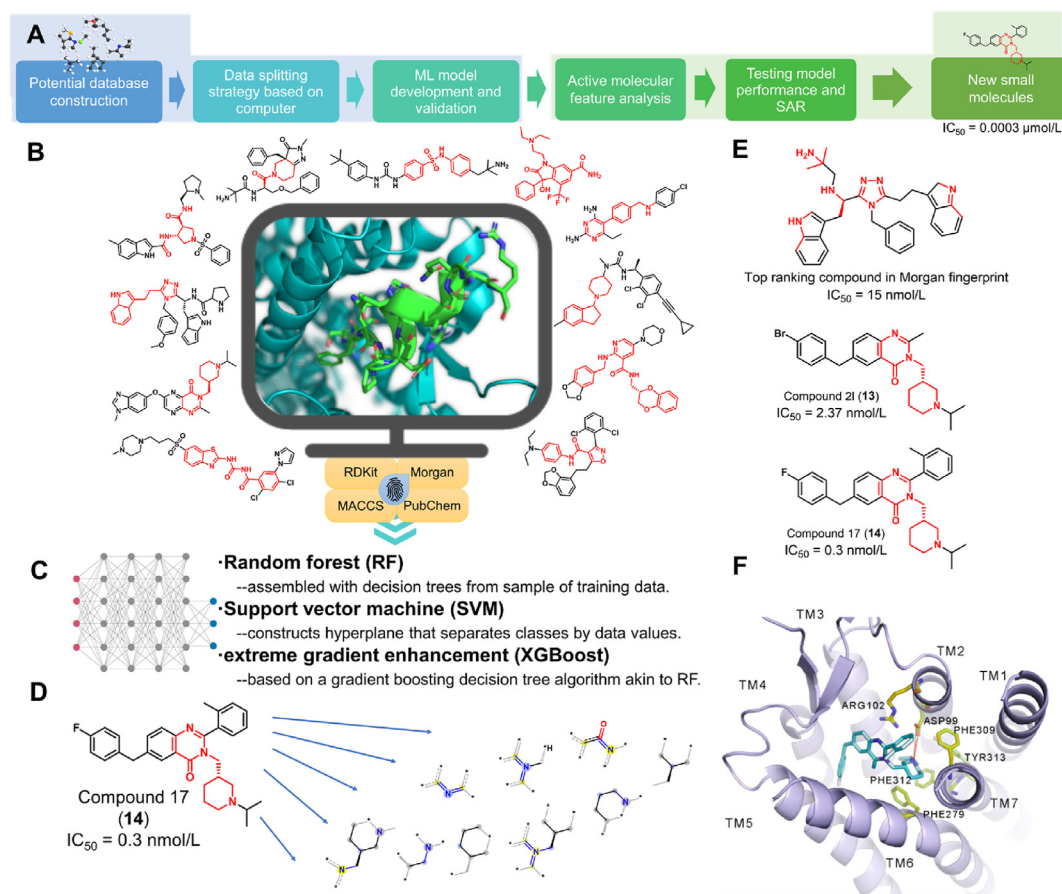
Figure 7 The discovery of small molecular ghrelin receptor inhibitors from peptides, analyzing and reconstructing using machine learning approaches. (A) The working flow of machine learning from peptides and peptidomimetics. (B) The structure of Ghrelin Receptor derived from peptide (light lime, ligand shown in green, respectively), with the SVM algorithm classifying key structure into different assays by similarity (structures around the computer icon, essential structural component shown in red). (C) After processed in machine learning model with Tanimoto coefficient algorithm, top ranked fragments were shown from Morgan fingerprint, the central atom and related bonds are marked as highlights. Figure was generated from BioRender.com. (D) Deconstruction of highly weighted features from final ghrelin receptor inhibitor candidate, compound 17 (**20**) with outstanding activity (IC_{50} = 0.3 nmol/L). The highly weighted features are validated and highlighted in red in the structure of the compound. (E) The structure of top ranking compound, compound 2l (**13**), and compound 17 (**14**). The core structure reveals similar relativity. (F) Co-crystal binding of GR and compound 17 (**20**), revealing predicted interactions with environment.

originally discovered manually and by cyber-intelligence. The SVM model correctly predicted the representative compound 17 and binding details in the pocket. Subsequent activity validation was outstanding (IC_{50} = 0.3 nmol/L). The docking model is derived from the crystal structure of GR (Fig. 7F, PDB ID: 6KO5)[175].

The ML model has paved a novel way to transform peptides into small molecules accurately and effectively. Liu et al. successfully demonstrated that ML is a reasonable approach to identifying outstanding small-molecule compound 17 (**20**) from a massive database[46]. However, there are still several aspects that need improvement. First, the foundation properties of the program, such as the size of the database, the variety of compound structures, and molecular fingerprints, considerably impact the model performance and should be optimized for a decent training process. Second, the sample constitution, combining peptides/peptidomimetics and small molecules, is favorable in this case, but the validation of models using peptides/peptidomimetics only requires further studies. In addition, the "one hot encode" method is sparse in high dimension, which means the codes of peptide/

peptidomimetic simulation structures might encumber the whole process. In cases with a huge library of binding molecules as the size of the training data significantly influences the performance of machine learning models, ML can still be beneficial in identifying exceptional small molecules.

3.3. Advanced in silico drug discovery for potent YAP-TEAD PPI disruptors: IAG-933 (**26**)

The Yes-Associated Protein (YAP) is one of the key effectors of the Hippo signaling pathway, which plays a crucial role in controlling organ size, tissue regeneration, and tumorigenesis[176–178]. However, in many cancers or tumors, this pathway is dysregulated, leading to the interaction of YAP with transcription factors such as Transcription Enhancer Associate Domain (TEAD) proteins[179–184]. This interaction activates the expression of genes involved in cell proliferation, survival, and stemness, promoting tumor growth and progression. Consequently, targeting the YAP−TEAD interaction has emerged as a promising therapeutic strategy for cancer treatment by inhibiting the oncogenic functions
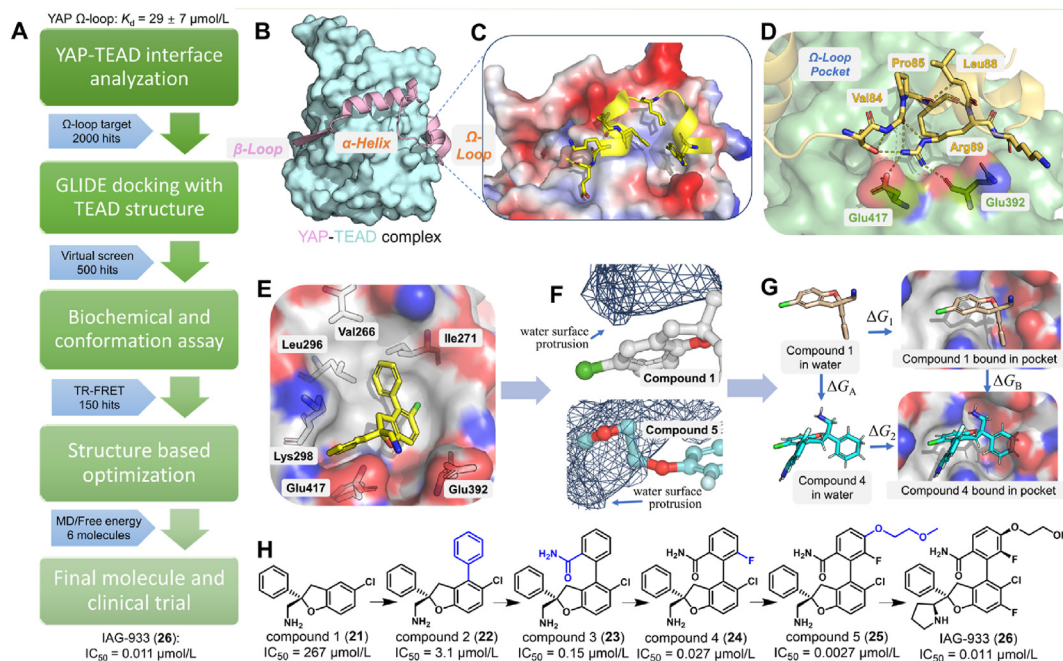
Figure 8 The discovery of small molecular YAP−TEAD inhibitors from PPI interface, designed and analyzed using novel tech aided approaches. (A) The design procedure from over 2000 virtual candidates to the final molecule IAG-933 which is under clinical trial. (B) YAP wrapping around the TEAD surface, YAP shown in pink and TEAD in teal blue. From left to right are β-loop, α-helix and Ω-loop. (C) The structure of YAP Ω-loop residues binding to TEAD pocket. (Red and blue areas represent oxygen and nitrogen binding sites, respectively). (D) Binding details of the TEAD Ω-loop pocket. (E) The binding pattern of compound 2 (**22**) with TEAD pocket. (F) WATMD analysis of solvent exposure, compound 2 (**22**) in top and compound 5 (**25**) in the bottom. (G) The schematic of free energy analysis of YAP−TEAD inhibitor compound series. (H) Structure of compound 1 (**21**) to IAG-933 (**26**).

of YAP in the Hippo pathway. In 2022−2023, the researches of Novartis published a series of researches on the discovery and optimization of YAP−TEAD PPI inhibitor IAG-933[54,55,185]. This small molecule inhibitor was reformed from a peptide hit and optimized using advanced *in silico* techniques to the clinical trial[53−55].

Between the YAP and TEAD, the interface is enormously extensive and slack that traditional druggable binding pockets are unable to be defined (Fig. 8A, PDB ID: 3KYS)[186−190]. The interface is mainly composed of three major parts from left to right on Fig. 8A: β-strand, α-helix, and Ω-loop[188]. The YAP binds to TEAD by wrapping across whole surface, thus small molecule drug discovery was impeded by untraceable direct binding pockets, leading peptides to be the more competitive druggable category[191−193]. Among this total 3500 Å^2 area, Furet et al. reported two shallow pockets separated by distance of 16 Å on the TEAD surface, one binds with YAP α-helix 61−73 amino acids, another binds with YAP Ω-loop 85−99 amino acids[55]. In previous research, Furet et al. discovered that the Ω-loop pocket manifests more affinity to become a more attractive target[52]. Subsequently, the researchers designed a series of potent linear 15-mer peptide inhibitors derived from the YAP Ω-loop sequence 85−99 using the structure-based design[52,194]. Based on the linear peptides' investigations, the team found that the Met 86 on the YAP Ω-loop can be replaced by a 6-chlorotryptophan for amplified affinity, thus conceptualized a high throughput virtual screening from the TEAD X-ray crystal structure (PDB ID:6Q36). Docking procedure with Novartis compound collection was performed with GLIDE using the core constraint setting, all structures were limited with obtaining either a 6-chloroindole or a chlorophenyl

moiety occupying the same position as the Met86 to mimic[195]. After the screening, the top 2000 molecules were visually inspected into a refined set of 500 compounds that binds to the Ω-loop appropriately. These around 500 compounds were firstly assessed in a TR-FRET assay for biochemical analyzation, affirming the inhibitory of YAP−TEAD PPI that identified approximately 150 compounds. Around 70 of them produced a chemical shift that indicated an active binding in the protein spectra secondly. Next, 2D [^{13}C,^{1}H]-HMQC spectra were applied to confirm the binding, giving out the first decent hit compound 1 (**21**) with around 180 μmol/L dissociation constant K_d. However, in the following X-ray structure analysis, dihydrobenzofuran core located at the bottom of the pocket revealed that the racemate compound 1 (**21**) cannot makes salt bridge interactions with residue Glu391^{TEAD4} (Glu392^{TEAD3}) and residue Glu417^{TEAD3} simultaneously in one enantiomer. Thus, the research team turned to subordinate compound 2 (**22**) as another attractive starting point, considering its diminutive volume and potential of selectivity to TEAD Ω-loop pocket. As shown in Fig. 8E, compound 2 (**22**) tends to disclose an unoccupied area which oriented toward position 4 of dihydrobenzofuran bicycle. Forming the upper border, residues Ile271, Leu296, Val266 are ideal binding positions for a phenyl group, because adequate van der Waals interactions can be formed without conformational strain. Added a phenyl group at the 4 position of compound 2 (**22**), gives the compound 3 (**23**) that shows amazingly 86-folds of affinity increase (**22**: IC$_{50}$ = 267 μmol/L, **23**: IC$_{50}$ = 3.1 μmol/L). Given that this affinity was based on only one face of the 4-phenyl substituent, the research team set off to add substituents on the 4-phenyl ring toward deeper site of the pocket. One ortho position

was introduced of amide group to make hydrogen bonds possible with backbone carbonyl oxygen atom of Gln270 and Lys274, resulting in a 21-fold increase of activity for compound 4 (**24**, IC_{50} = 150 nmol/L). Another ortho position was added with a small fluorine substituent to compound 5 (**25**), with an IC_{50} value of 27 nmol/L. Finally for the meta position, the research team applied the Amber MD suite for molecular dynamic simulation to seek improved solubility[196,197]. The structure of TEAD3 (PDB ID: 8A0V) was used to dock with small molecules **21**-**25** under ff19SB forcefield and TIP3P water model and 3D-RISM solvent system[198−201]. At the meta position, a 2-methoxyethoxy substituent was added which can improve the interaction with solvent surface of compound 5 (**25**), confirmed by WATMD tool developed by Novartis shown in Fig. 8F [202,203]. Along the optimization of YAP−TEAD inhibitors to achieve a terrific IC_{50} value of 2.7 nmol/L of compound 5 (**25**), the research team performed alchemical binding free energy calculations using relative and absolute binding free energy techniques in Amber20[204−206]. Exemplary for relative binding free energy (RBFE) calculations. As shown in Fig. 8G, within a classic thermodynamic cycle combined with RDKit to align structural similarity from small molecule **22** to **25**, a perturbation map was then created to set up the calculations and a graph was assembled using NetworkX[207].

As a successful small molecule transformed from the YAP peptide sequence, compound 5 (**25**) was further optimized to IAG-933 (**26**), with improved binding and selectivity as well as pharmacokinetic properties that IAG-933 (**26**) can be successfully promoted into clinical trials. In the latest research, Furet et al. confirmed its inhibitory toward the PPI of YAP−TEAD in a rapid way through destructing the coactivators binding[56]. And pharmacological bioassay of IAG-933 (**26**) demonstrated directly and selectively pharmacological disruption of the YAP−TEAD interface by inhibiting Hippo-dependent and RAS−MAPK-altered cancers[56]. Being a novel approach guided by *in silico* screen-GLIDE docking-MD simulated binding assay, these researches paved a way of discovering wide and shallow pockets that were once impossible for small molecules. As the IAG-933 (**26**) is under phase I clinical trial, it strongly proved that certain peptides with clear co-crystal structures and appropriate binding sites can be transformed into small molecules.

4. Conclusions and perspectives

Recent research optimizing peptides to small molecules can be primarily categorized into classical and novel designs. The case of compound 14 (**5**) revealed a step-by-step train of thought; compound 7 (**6**) introduced the dual-action design to combine ordinary function with peptide mimicry; GC-376 (**8**) inspired rational design based on interfaces, and compound 12b (**11**) indicated that the sequence of a peptide can be investigated to shrink into small molecules. Additionally, compound 2l (**18**), conducted under the guidance of the EKO theory, demonstrated a more advanced approach to designing and evaluating small-molecule peptidomimetics from numerous peptide templates. Compound 17 (**20**) proved that ML and AI can be used to accelerate the whole process like never before. In second configuration, novel techniques are more involved in the drug discovery process and replaced the deduction of traditional way with new evidence and power of computational machines. Various methods can be applied to different peptides and situations. For macrocyclic peptides providing clear X-ray structures, a classical design involving cocrystal analysis is suitable. Key interfaces of large peptides can

be analyzed using ML, and small peptides can be fragmented and simulated by small molecules. For many native peptides binding to the same target, the EKO strategy can summarize commonalities to determine the overlapping segments and guide the design of small molecules. If the binding peptide can be sampled into the database, then the ML method will help find the essential small-molecule structure. In a general perspective, as shown in Fig. 9, the process can be described in four stages.

Stage I: From native peptides to potential molecules and optimized small molecules: Classic approaches involve collecting information from peptide sequence, properties, and structures to identify characteristics of peptidomimetics presenting. Medicinal chemists utilize methods like alanine scanning and X-ray co-structure. Computational approaches enable large-scale data processing with HTS, virtual screening, EKO, etc.

Stage II: From primary peptidomimetics to active peptides: To slim the scaffold, residue deletion or replacement with a heterocyclic ring of scaffolds is used to define active scaffolds. Computational measures involve algorithms and theories like AMBER, GROningen MAchine for Chemical Simulations, and GIST to assist in defining active scaffolds with properties and activity because these algorithms and theories are based on a systematical mechanism that is suitable for optimizing solvation and binding forcefield.

Stage III: From active scaffolds to potential molecules that mimic the special secondary conformation of peptides: Classic approaches suggest the use of NMR, cocrystal, and cyclic constraints for identifying potential molecules. Computers present peptide structural information with different fingerprints and/or docking guidance from deep learning.

Stage IV: From potential molecules to further optimized active molecules: Ordinarily, strategies like SAR studies in pharmacophore replacement and redesign after checking are used to identify the best binding pattern and interactions. Meanwhile, computational intelligence programs, including SiteMap, QSAR studies, integrated learning, and dynamic molecular mechanics, enable multitasking in activity enhancement to finally obtain small molecules derived from certain peptides.

As time went on, the strategy of optimizing peptides into small molecules evolves tremendously from the first peptide insulin used as drug in 1923 to present time 2024 when Google DeepMind laboratory just announced new version of ground-breaking AlphaFold3 in Fig. 9. Traditional methods have areas for improvement, including high overheads in time and cost, complexity, randomization during processes, and uncertainty of inspiration. With the development of various disciplines, new ideas and techniques drive advances in medicinal chemistry approaches, optimizing peptides into small molecules. Rational analysis raised by researchers like Yoshida helps identify interactions for small-molecule mimicry, while ML algorithms expedite peptide library collection and potential scaffold designing. In an optimistic outlook, this field of research might soon be widely popular and utilized by researchers from pharmaceutical chemistry, pharmacology, and biology[39,50,51]. Accumulating experiences can further expand drug sources and better optimize drug forms. Novel techniques can complement the deficiency of traditional design in analyzing binding patterns and generating substituent groups. Additional peptides can be developed into small molecules to improve druggability and integrated functions across multiple targets. Nevertheless, there are still problems and deficiencies that remain to be addressed. The current detection in chemical property evaluations requires higher
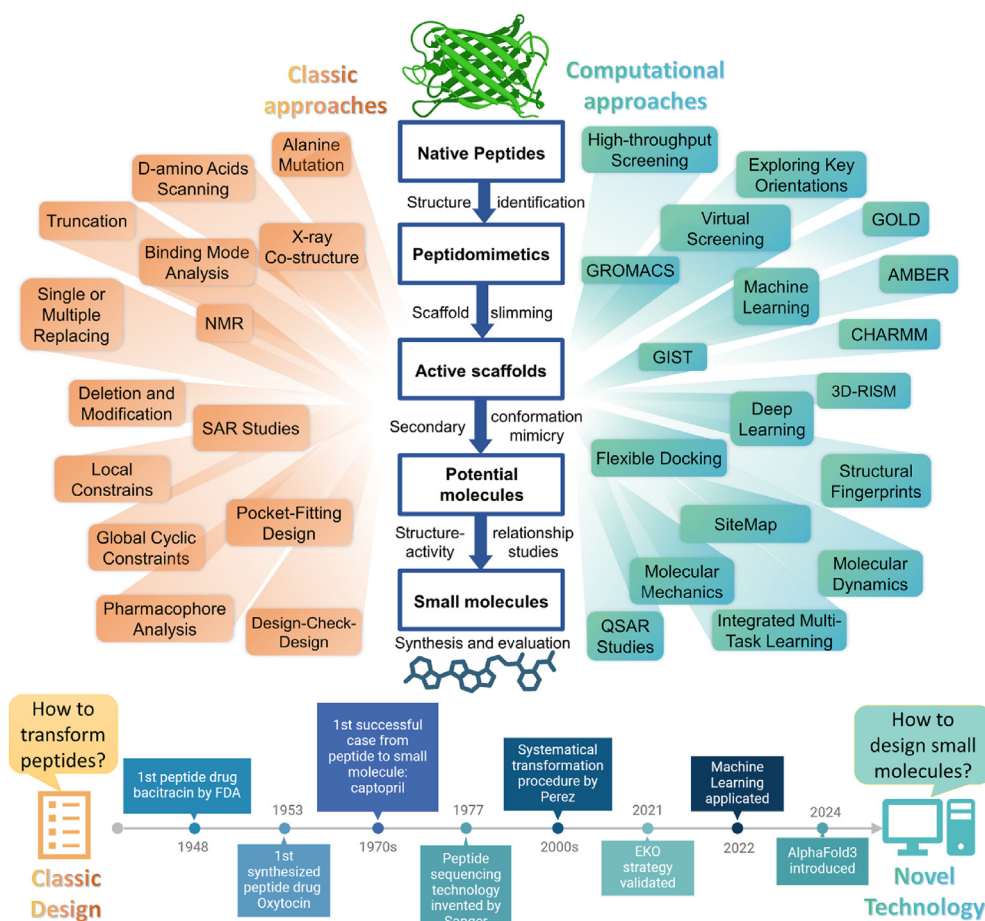
Figure 9 Universal strategy and available technologies from identifying peptides to transformation of small molecules, and the timeline of special event on the road from peptides to small molecules.

precision for theoretical corresponding, and secondary conformational optimization necessitates a comprehensive understanding of particular peptides and binding pockets. Developing capabilities in key fragment identification and small molecular model refinement will enable medicinal chemists to "transform" peptides into small molecules with additional cutting-edge technology, a much-shortened drug development process, and better-achieved therapeutic effects. Furthermore, this field of research will guide additional aspects like small molecular ligand warhead design, peptidomimetic target discovery, and diagnostic reagent or biomarker development.

Peptide-to-small-molecule (PTSM) strategy is a way of condensation of large peptide, while the fragment-based-drug-design (FBDD) is the other solution to expand a core fragment hit to large molecules. They are two perspectives to the same topic—drug discovery and optimization. Drug hits are random and unpredictable, both peptides and small molecules are often taken into account in drug discovery. And next step for optimization, PTSM takes a crucial part working on a peptide template maintaining its activity and bioavailability to improve the ADMET properties, etc. The FBDD obtain more binding effects while preserving the small molecule scaffold core. As described in part 2.1 Yoshida's case, starting with a peptide display to obtain peptide hits with decent affinity *in vitro*, with a series of cocrystal studies to determine the pharmacophore docking-optimization process, to small molecules[39]. And in part 3.2 the case of

Wenjie Liu, a potential database was established with peptide and molecular fragments[46]. This *in silico* process excluded traditional approaches of design-check-redesign cycle, instead the structures were stored with data packages and processed by computers and algorithms, to output the final small molecule.

The first advantages of the PTSM strategy are the accelerated peptide hit discovery process from large peptide screening database, while more "hard-to-drug" targets can be included. Second, is the more comprehensive understanding of the binding sites thanks to the large peptide hit that reveals the induced-fit pocket information for *de novo* design to follow. Concluded from the cases above, to applicate the PTSM strategy, a peptide screening platform is needed in the first place, *in vitro* or *in silico* are all suitable. Next, a cocrystal structure analysis or cyto-EM can be included to provide a solid basis for binding pattern studies, to guide the following optimization. The third step requires a decent structure-based design and optimization toward final small molecule drug. Challenges will be more diversified and intricate, as peptides are unable to convey the exactly properties into small molecules and obstacles optimizing chemical structures. However as for the opportunities, the computer-aided-drug-design (CADD) and artificial-intelligence-drug-design (AIDD) is clearly thriving along with the artificial intelligence and machine learning market. The Generative Pre-trained Transformer engines that collect pathway signaling information from disease phenotypes, AlphaFold 3 that convert the sequence into predicted protein

structures, and molecular scaffold generative algorithms to grow hit molecules with more binding sites. In parallel, the PTSM strategy will draw more importance in the next era of computational time.

Acknowledgments

Author contributions

Zeyu Han: Writing − original draft. Zekai Shen: Software. Jiayue Pei: Formal analysis. Qidong You: Data curation. Qiuyue Zhang: Investigation. Lei Wang: Writing − review & editing.

Conflicts of interest

The authors declare that they have no known competing financial interests or personal relationships that could have appeared to influence the work reported in this paper.

References

1. Fosgerau K, Hoffmann T. Peptide therapeutics: current status and future directions. *Drug Discov Today* 2015;**20**:122−8.
2. Zhao L, Zhao J, Zhong K, Tong A, Jia D. Targeted protein degradation: mechanisms, strategies and application. *Signal Transduct Target Ther* 2022;**7**:113.
3. Békés M, Langley DR, Crews CM. Protac targeted protein degraders: the past is prologue. *Nat Rev Drug Discov* 2022;**21**:181−200.
4. Hanzl A, Winter GE. Targeted protein degradation: current and future challenges. *Curr Opin Chem Biol* 2020;**56**:35−41.
5. Dale B, Cheng M, Park KS, Kaniskan HÜ, Xiong Y, Jin J. Advancing targeted protein degradation for cancer therapy. *Nat Rev Cancer* 2021;**21**:638−54.
6. Henninot A, Collins JC, Nuss JM. The current state of peptide drug discovery: back to the future?. *J Med Chem* 2018;**61**:1382−414.
7. Beck H, Harter M, Hass B, Schmeck C, Baerfacker L. Small molecules and their impact in drug discovery: a perspective on the occasion of the 125th anniversary of the Bayer Chemical Research Laboratory. *Drug Discov Today* 2022;**27**:1560−74.
8. Pennington LD, Muegge I. Holistic drug design for multiparameter optimization in modern small molecule drug discovery. *Bioorg Med Chem Lett* 2021;**41**:128003.
9. Craik DJ, Fairlie DP, Liras S, Price D. The future of peptide-based drugs. *Chem Biol Drug Des* 2012;**81**:136−47.
10. Lin L, Chi J, Yan Y, Luo R, Feng X, Zheng Y, et al. Membrane-disruptive peptides/peptidomimetics-based therapeutics: promising systems to combat bacteria and cancer in the drug-resistant era. *Acta Pharm Sin B* 2021;**11**:2609−44.
11. Otvos L Jr, Wade JD. Big peptide drugs in a small molecule world. *Front Chem* 2023;**11**:1302169.
12. Hashimoto C, Eichler J. Turning peptide ligands into small-molecule inhibitors of protein−protein interactions. *Chembiochem* 2015;**16**:1855−6.
13. Brytan W, Padrela L. Structural modifications for the conversion of proteins and peptides into stable dried powder formulations: a review. *J Drug Deliv Sci Technol* 2023;**89**:104992.
14. Lai Y, Chu X, Di L, Gao W, Guo Y, Liu X, et al. Recent advances in the translation of drug metabolism and pharmacokinetics science for drug discovery and development. *Acta Pharm Sin B* 2022;**12**:2751−77.
15. Nemec K, Schubert-Zsilavecz M. Vom Teprotid zum Captopril. Rationales Design von ACE-Hemmern [From teprotide to captopril. Rational design of ACE inhibitors]. *Pharm Unserer Zeit* 2003;**32**:11−6.
16. DiBianco R. Adverse reactions with angiotensin converting enzyme (ACE) inhibitors. *Med Toxicol* 1986;**1**:122−41.
17. Duncia JV, Chiu AT, Carini DJ, Gregory GB, Johnson AL, Price WA, et al. The discovery of potent nonpeptide angiotensin II receptor antagonists: a new class of potent antihypertensives. *J Med Chem* 1990;**33**:1312−29.
18. Smeby RR, Fermandjian S. Conformation of angiotensin II. In: Weinstein B, editor. *Chemistry and biochemistry of amino acids, peptides and proteins*. 5th ed. New York: Marcel Dekker; 1978. p. 177.
19. Bormann T, Maus R, Stolper J, Jonigk D, Welte T, Gauldie J, et al. Role of the COX2−PGE$_2$ axis in *S. pneumoniae*-induced exacerbation of experimental fibrosis. *Am J Physiol Lung Cel Mol Physiol* 2021;**320**:L377−92.
20. Bingham CO, 3rd. Development and clinical application of COX-2-selective inhibitors for the treatment of osteoarthritis and rheumatoid arthritis. *Cleve Clin J Med* 2002;**69**(Suppl 1):SI5−12.
21. Noveck RJ, Hubbard RC. Parecoxib sodium, an injectable COX-2-specific inhibitor, does not affect unfractionated heparin-regulated blood coagulation parameters. *J Clin Pharmacol* 2004;**44**:474−80.
22. Dalpiaz AS, Peterson D. Parecoxib: a shift in pain management?. *Expert Rev Neurother* 2004;**4**:165−77.
23. Del Gatto A, Cobb SL, Zhang J, Zaccaro L. Editorial: peptidomimetics: synthetic tools for drug discovery and development. *Front Chem* 2021;**9**:802120.
24. Lubell WD. Peptidomimetics I. New York: Springer,2017.
25. Mabonga L, Kappo AP. Peptidomimetics: a synthetic tool for inhibiting protein−protein interactions in cancer. *Int J Pept Res Ther* 2019;**26**:225−41.
26. Mendez-Samperio P. Peptidomimetics as a new generation of antimicrobial agents: current progress. *Infect Drug Resist* 2014;**7**:229−37.
27. Cai J, Wei L. Editorial of special column "novel peptides and peptidomimetics in drug discovery". *Acta Pharm Sin B* 2021;**11**:2606−8.
28. Trabocchi A. Principles and applications of small molecule peptidomimetics. In: Trabocchi A, Lenci E, editors. *Small molecule drug discovery*. New York: Elsevier; 2020. p. 163−95.
29. Sawyer TK. Peptidomimetic and nonpeptide drug discovery: receptor, protease, and signal transduction therapeutic targets. In: Taylor JB, Triggle DJ, editors. *Comprehensive medicinal chemistry II*. New York: Elsevier; 2007. p. 603−47.
30. Matyjaszewski K, Moller M. *Polymer science: a comprehensive reference*. New York: Elsevier; 2012.
31. Erak M, Bellmann-Sickert K, Els-Heindl S, Beck-Sickinger AG. Peptide chemistry toolbox_Transforming natural peptides into peptide therapeutics. *Bioorg Med Chem* 2018;**26**:2759−65.
32. Zhu J, Wang J, Han W, Xu D. Neural relational inference to learn long-range allosteric interactions in proteins from molecular dynamics simulations. *Nat Commun* 2022;**13**:1661.
33. Zhou W, Liu Y, Li H, Song Z, Ma Y, Zhu Y. Mass spectrometry and computer simulation predict the interactions of AGPS and HNRNPK in glioma. *BioMed Res Int* 2021;**2021**:6181936.
34. Xin D, Ko E, Perez LM, Ioerger TR, Burgess K. Evaluating minimalist mimics by exploring key orientations on secondary structures (EKOS). *Org Biomol Chem* 2013;**11**:7789−801.
35. Imai K, Shimizu K, Honda H. Machine learning screening of bile acid-binding peptides in a peptide database derived from food proteins. *Sci Rep* 2021;**11**:16123.

36. Basith S, Manavalan B, Hwan Shin T, Lee G. Machine intelligence in peptide therapeutics: a next-generation tool for rapid disease screening. *Med Res Rev* 2020;**40**:1276−314.

37. Ren Z, Zhang Z, Wei J, Dong B, Lee C. Wavelength-multiplexed hook nanoantennas for machine learning enabled mid-infrared spectroscopy. *Nat Commun* 2022;**13**:3859.

38. Li Petri G, Di Martino S, De Rosa M. Peptidomimetics: an overview of recent medicinal chemistry efforts toward the discovery of novel small molecule inhibitors. *J Med Chem* 2022;**65**:7438−75.

39. Yoshida S, Uehara S, Kondo N, Takahashi Y, Yamamoto S, Kameda A, et al. Peptide-to-small molecule: a pharmacophore-guided small molecule lead generation strategy from high-affinity macrocyclic peptides. *J Med Chem* 2022;**65**:10655−73.

40. Sun K, Ding Z, Jia X, Cheng H, Li Y, Wu Y, et al. Extracellular disintegration of viral proteins as an innovative strategy for developing broad-spectrum antivirals against coronavirus. *CCS Chem* 2024;**6**:487−96.

41. Bai B, Belovodskiy A, Hena M, Kandadai AS, Joyce MA, Saffran HA, et al. Peptidomimetic α-acyloxymethylketone warheads with six-membered lactam P1 glutamine mimic: SARS-CoV-2 3CL protease inhibition, coronavirus antiviral activity, and *in vitro* biological stability. *J Med Chem* 2022;**65**:2905−25.

42. Fu L, Ye F, Feng Y, Yu F, Wang Q, Wu Y, et al. Both Boceprevir and GC376 efficaciously inhibit SARS-CoV-2 by targeting its main protease. *Nat Commun* 2020;**11**:4417.

43. Sacco MD, Ma C, Lagarias P, Gao A, Townsend JA, Meng X, et al. Structure and inhibition of the SARS-CoV-2 main protease reveal strategy for developing dual inhibitors against M^{pro} and cathepsin l. *Sci Adv* 2020;**6**:eabe0751.

44. Ma C, Sacco MD, Hurst B, Townsend JA, Hu Y, Szeto T, et al. Boceprevir, GC-376, and calpain inhibitors II, XII inhibit SARS-CoV-2 viral replication by targeting the viral main protease. *Cell Res* 2020;**30**:678−92.

45. Rathnayake AD, Zheng J, Kim Y, Perera KD, Mackin S, Meyerholz DK, et al. 3c-like protease inhibitors block coronavirus replication *in vitro* and improve survival in MERS-CoV-infected mice. *Sci Transl Med* 2020;**12**:eabc5332.

46. Liu W, Hopkins AM, Yan P, Du S, Luyt LG, Li Y, et al. Can machine learning 'transform' peptides/peptidomimetics into small molecules? A case study with ghrelin receptor ligands. *Mol Divers* 2023;**27**:2239−55.

47. Kerr RV, Fairbairn JA, Merritt AT, Bugg TDH. Peptidomimetic analogues of an Arg-Trp-x-x-Trp motif responsible for interaction of translocase MraY with bacteriophage varphiX174 lysis protein E. *Bioorg Med Chem* 2021;**52**:116502.

48. Rodolis MT, Mihalyi A, O'Reilly A, Slikas J, Roper DI, Hancock RE, et al. Identification of a novel inhibition site in translocase MraY based upon the site of interaction with lysis protein E from bacteriophage varphiX174. *Chembiochem* 2014;**15**:1300−8.

49. Lyu RL, Joy S, Packianathan C, Laganowsky A, Burgess K. Small molecule peptidomimetic trypsin inhibitors: validation of an EKO binding mode, but with a twist. *Org Biomol Chem* 2022;**20**:2075−80.

50. Tedesco F, Calugi L, Lenci E, Trabocchi A. Peptidomimetic small-molecule inhibitors of 3clpro activity and spike−ACE2 interaction: toward dual-action molecules against coronavirus infections. *J Org Chem* 2022;**87**:12041−51.

51. Yoshida S, Sako Y, Nikaido E, Ueda T, Kozono I, Ichihashi Y, et al. Peptide-to-small molecule: discovery of non-covalent, active-site inhibitors of β-herpesvirus proteases. *ACS Med Chem Lett* 2023;**14**:1558−66.

52. Hau JC, Erdmann D, Mesrouze Y, Furet P, Fontana P, Zimmermann C, et al. The tead4−YAP/TAZ protein−protein interaction: expected similarities and unexpected differences. *Chembiochem* 2013;**14**:1218−25.

53. Sellner H, Chapeau E, Furet P, Voegtle M, Salem B, Le Douget M, et al. Optimization of a class of dihydrobenzofurane analogs toward orally efficacious YAP-TEAD protein−protein interaction inhibitors. *ChemMedChem* 2023;**18**:e202300051.

54. Awoonor-Williams E, Dickson CJ, Furet P, Golosov AA, Hornak V. Leveraging advanced *in silico* techniques in early drug discovery: a study of potent small-molecule YAP−TEAD PPI disruptors. *J Chem Inf Model* 2023;**63**:2520−31.

55. Furet P, Bordas V, Le Douget M, Salem B, Mesrouze Y, Imbach-Weese P, et al. The first class of small molecules potently disrupting the YAP−TEAD interaction by direct competition. *ChemMedChem* 2022;**17**:e202200303.

56. Chapeau EA, Sansregret L, Galli GG, Chene P, Wartmann M, Mourikis TP, et al. Direct and selective pharmacological disruption of the YAP−TEAD interface by IAG933 inhibits Hippo-dependent and RAS−MAPK-altered cancers. *Nat Cancer* 2024. https://doi.org/10.1038/s43018-024-00754-9.

57. Roberti A, Fernandez AF, Fraga MF. Nicotinamide *N*-methyltransferase: at the crossroads between cellular metabolism and epigenetic regulation. *Mol Metab* 2021;**45**:101165.

58. Wang W, Yang C, Wang T, Deng H. Complex roles of nicotinamide *N*-methyltransferase in cancer progression. *Cell Death Dis* 2022;**13**:267.

59. van Haren MJ, Zhang Y, Thijssen V, Buijs N, Gao Y, Mateuszuk L, et al. Macrocyclic peptides as allosteric inhibitors of nicotinamide *N*-methyltransferase (NNMT). *RSC Chem Biol* 2021;**2**:1546−55.

60. Kashiwagi K, Reid PC. World Intellectual Property Organization. Rapid display method in translational synthesis of peptide. International patent WO2011049157. 2010 Oct 21.

61. Kelly CM, Gutierrez Sainz L, Chi P. The management of metastatic GIST: current standard and investigational therapeutics. *J Hematol Oncol* 2021;**14**:2.

62. Waibl F, Kraml J, Hoerschinger VJ, Hofer F, Kamenik AS, Fernandez-Quintero ML, et al. Grid inhomogeneous solvation theory for cross-solvation in rigid solvents. *J Chem Phys* 2022;**156**:204101.

63. Nguyen CN, Young TK, Gilson MK. Grid inhomogeneous solvation theory: hydration structure and thermodynamics of the miniature receptor cucurbit[7]uril. *J Chem Phys* 2012;**137**:044101.

64. Jung SW, Kim M, Ramsey S, Kurtzman T, Cho AE. Water pharmacophore: designing ligands using molecular dynamics simulations with water. *Sci Rep* 2018;**8**:10400.

65. Wang L, Berne BJ, Friesner RA. Ligand binding to protein-binding pockets with wet and dry regions. *Proc Natl Acad Sci U S A* 2011;**108**:1326−30.

66. Ichihara O, Shimada Y, Yoshidome D. The importance of hydration thermodynamics in fragment-to-lead optimization. *ChemMedChem* 2014;**9**:2708−17.

67. Krishnakumar HN, Momtaz DA, Sherwani A, Mhapankar A, Gonuguntla RK, Maleki A, et al. Pathogenesis and progression of anosmia and dysgeusia during the COVID-19 pandemic. *Eur Arch Oto-Rhino-Laryngol* 2023;**280**:505−9.

68. Wu F, Zhao S, Yu B, Chen YM, Wang W, Song ZG, et al. A new coronavirus associated with human respiratory disease in China. *Nature* 2020;**579**:265−9.

69. Robinson PC, Liew DFL, Tanner HL, Grainger JR, Dwek RA, Reisler RB, et al. COVID-19 therapeutics: challenges and directions for the future. *Proc Natl Acad Sci U S A* 2022;**119**:e2119893119.

70. Qin Z, Dong B, Wang R, Huang D, Wang J, Feng X, et al. Preparing anti-SARS-CoV-2 agent EIDD-2801 by a practical and scalable approach, and quick evaluation *via* machine learning. *Acta Pharm Sin B* 2021;**11**:3678−82.

71. Rahman S, Montero MTV, Rowe K, Kirton R, Kunik Jr F. Epidemiology, pathogenesis, clinical presentations, diagnosis and treatment of COVID-19: a review of current evidence. *Expert Rev Clin Pharmacol* 2021;**14**:601−21.

72. El Karoui K, De Vriese AS. COVID-19 in dialysis: clinical impact, immune response, prevention, and treatment. *Kidney Int* 2022;**101**:883−94.

73. Xiu S, Dick A, Ju H, Mirzaie S, Abdi F, Cocklin S, et al. Inhibitors of SARS-CoV-2 entry: current and future opportunities. *J Med Chem* 2020;**63**:12256−74.

74. Ghosh AK, Brindisi M, Shahabi D, Chapman ME, Mesecar AD. Drug development and medicinal chemistry efforts toward SARS-coronavirus and COVID-19 therapeutics. *ChemMedChem* 2020;**15**: 907−32.

75. Liu Y, Liang C, Xin L, Ren X, Tian L, Ju X, et al. The development of coronavirus 3C-Like protease (3CL^pro) inhibitors from 2010 to 2020. *Eur J Med Chem* 2020;**206**:112711.

76. Hu Q, Xiong Y, Zhu GH, Zhang YN, Zhang YW, Huang P, et al. The SARS-CoV-2 main protease (M^pro): structure, function, and emerging therapies for COVID-19. *MedComm* 2020;**2022**:e151.

77. Han J, Perez J, Schafer A, Cheng H, Peet N, Rong L, et al. Influenza virus: small molecule therapeutics and mechanisms of antiviral resistance. *Curr Med Chem* 2018;**25**:5115−27.

78. Xiang H, Zhou M, Li Y, Zhou L, Wang R. Drug discovery by targeting the protein−protein interactions involved in autophagy. *Acta Pharm Sin B* 2023;**13**:4373−90.

79. Serwetnyk MA, Blagg BSJ. The disruption of protein−protein interactions with co-chaperones and client substrates as a strategy towards Hsp90 inhibition. *Acta Pharm Sin B* 2021;**11**:1446−68.

80. Wang X, Yang C, Sun Y, Sui X, Zhu T, Wang Q, et al. A novel screening strategy of anti-SARS-CoV-2 drugs *via* blocking interaction between spike RBD and ACE2. *Environ Int* 2021;**147**:106361.

81. Lai HTT, Nguyen LH, Phan AD, Kranjc A, Nguyen TT, Nguyen-Manh D. A comparative study of receptor interactions between SARS-CoV and SARS-CoV-2 from molecular modeling. *J Mol Model* 2022;**28**:305.

82. Veeramachaneni GK, Thunuguntla V, Bobbillapati J, Bondili JS. Structural and simulation analysis of hotspot residues interactions of SARS-CoV 2 with human ACE2 receptor. *J Biomol Struct Dyn* 2021; **39**:4015−25.

83. Ullrich S, Nitsche C. The SARS-CoV-2 main protease as drug target. *Bioorg Med Chem Lett* 2020;**30**:127377.

84. Paul A, Sarkar A, Saha S, Maji A, Janah P, Kumar Maity T. Synthetic and computational efforts towards the development of peptidomimetics and small-molecule SARS-CoV 3CLpro inhibitors. *Bioorg Med Chem* 2021;**46**:116301.

85. Kronenberger T, Laufer SA, Pillaiyar T. COVID-19 therapeutics: small-molecule drug development targeting SARS-CoV-2 main protease. *Drug Discov Today* 2023;**28**:103579.

86. Valdivielso AM, Ventosa-Andrés P, García-López MT, Herranz R, Gutiérrez-Rodríguez M. Synthesis and regioselective functionalization of piperazin-2-ones based on Phe-Gly pseudodipeptides. *Eur J Org Chem* 2013;**2013**:155−61.

87. Yan R, Zhang Y, Li Y, Xia L, Guo Y, Zhou Q. Structural basis for the recognition of SARS-CoV-2 by full-length human ACE2. *Science* 2020;**367**:1444−8.

88. Larue RC, Xing E, Kenney AD, Zhang Y, Tuazon JA, Li J, et al. Rationally designed ACE2-derived peptides inhibit SARS-CoV-2. *Bioconjug Chem* 2021;**32**:215−23.

89. Trabocchi A, Menchi G, Danieli E, Guarna A. Synthesis of a bicyclic delta-amino acid as a constrained Gly-Asn dipeptide isostere. *Amino Acids* 2008;**35**:37−44.

90. Maligres PE, Waters MS, Weissman SA, McWilliams JC, Lewis S, Cowen J, et al. Preparation of a clinically investigated ras farnesyl transferase inhibitor. *J Heterocyclic Chem* 2003;**40**:229−41.

91. Kitamura S, Fukushi H, Miyawaki T, Kawamura M, Konishi N, Terashita ZI, et al. Potent dibasic GPIIb/IIIa antagonists with reduced prolongation of bleeding time: synthesis and pharmacological evaluation of 2-oxopiperazine derivatives. *J Med Chem* 2001;**44**: 2438−50.

92. Tabatabaei MS, Ahmed M. Enzyme-linked immunosorbent assay (ELISA). *Methods Mol Biol* 2022;**2508**:115−34.

93. Khodadadi A, Madani R, Hoghooghi Rad N, Atyabi N. Development of nano-ELISA method for serological diagnosis of toxoplasmosis in mice. *Arch Razi Inst* 2021;**75**:419−26.

94. Cao Y, Wang J, Jian F, Xiao T, Song W, Yisimayi A, et al. Omicron escapes the majority of existing SARS-CoV-2 neutralizing antibodies. *Nature* 2022;**602**:657−63.

95. Imran M, Thabet HK, Alaqel SI, Alzahrani AR, Abida A, Alshammari MK, et al. The therapeutic and prophylactic potential of quercetin against COVID-19: an outlook on the clinical studies, inventive compositions, and patent literature. *Antioxidants* 2022;**11**: 876.

96. Natesh J, Mondal P, Penta D, Abdul Salam AA, Meeran SM. Culinary spice bioactives as potential therapeutics against SARS-CoV-2: computational investigation. *Comput Biol Med* 2021;**128**:104102.

97. Pelay-Gimeno M, Glas A, Koch O, Grossmann TN. Structure-based design of inhibitors of protein−protein interactions: mimicking peptide binding epitopes. *Angew Chem Int Ed Engl* 2015;**54**: 8896−927.

98. Zhu J, Zhang H, Lin Q, Lyu J, Lu L, Chen H, et al. Progress on SARS-CoV-2 3CLpro inhibitors: inspiration from SARS-CoV 3CLpro peptidomimetics and small-molecule anti-inflammatory compounds. *Drug Des Devel Ther* 2022;**16**:1067−82.

99. Yadav R, Chaudhary JK, Jain N, Chaudhary PK, Khanra S, Dhamija P, et al. Role of structural and non-structural proteins and therapeutic targets of SARS-CoV-2 for COVID-19. *Cells* 2021;**10**: 821.

100. Reina J, Iglesias C. Nirmatrelvir plus ritonavir (Paxlovid) a potent SARS-CoV-2 3CLpro protease inhibitor combination. *Rev Esp Quimioter* 2022;**35**:236−40.

101. Chang K-O, Kim Y, Groutas WC, Perlman S, Univ Kansas State, Univ Wichita State, Univ Iowa Res Found.S. Broad spectrum antivirals against coronavirus. International patent WO2021202460. 2021 Oct 07.

102. Kim Y, Lovell S, Tiew KC, Mandadapu SR, Alliston KR, Chang KO, et al. Broad-spectrum antivirals against 3C or 3C-like proteases of picornaviruses, noroviruses, and coronaviruses. *J Virol* 2012;**86**: 11754−62.

103. Anand K, Ziebuhr J, Wadhwani P, Mesters JR, Hilgenfeld R. Coronavirus main proteinase (3CLpro) structure: basis for design of anti-SARS drugs. *Science* 2003;**300**:1763−7.

104. Luan XD, Chen BX, Shang WJ, Yin WC, Jin Y, Zhang LK, et al. Structure basis for inhibition of SARS-CoV-2 by the feline drug GC376. *Acta Pharmacol Sin* 2022;**44**:255−7.

105. Ko E, Liu J, Perez LM, Lu G, Schaefer A, Burgess K. Universal peptidomimetics. *J Am Chem Soc* 2011;**133**:462−77.

106. Ambrus G, Whitby LR, Singer EL, Trott O, Choi E, Olson AJ, et al. Small molecule peptidomimetic inhibitors of importin alpha/beta mediated nuclear transport. *Bioorg Med Chem* 2010;**18**: 7611−20.

107. Marshall GR. A hierarchical approach to peptidomimetic design. *Tetrahedron* 1993;**49**:3547−58.

108. Nakayoshi T, Kato K, Kurimoto E, Oda A. Virtual alanine scan of the main protease active site in severe acute respiratory syndrome coronavirus 2. *Int J Mol Sci* 2021;**22**:9837.

109. Ma KH, Guo YJ, Wang L, Tong NH. Projective-truncation-approximation study of the one-dimensional varphi;4 lattice model. *Phys Rev E* 2022;**106**:014110.

110. Wilkinson J, Huang JY, Marsden A, Harhay MO, Vail A, Roberts SA. The implications of outcome truncation in reproductive medicine RCTs: a simulation platform for trialists and simulation study. *Trials* 2021;**22**:520.

111. Chen H, Alexander-Katz A. Polymer-based catch-bonds. *Biophys J* 2011;**100**:174−82.

112. Nazzaro A, Lu B, Sawyer N, Watkins AM, Arora PS. Macrocyclic beta-sheets stabilized by hydrogen bond surrogates. *Angew Chem Int Ed Engl* 2023;**62**:e202303943.

113. Agouram N, El Hadrami EM, Bentama A. 1,2,3-Triazoles as biomimetics in peptide science. *Molecules* 2021;**26**:2937.

114. Perez JJ, Perez RA, Perez A. Computational modeling as a tool to investigate PPI: from drug design to tissue engineering. *Front Mol Biosci* 2021;**8**:681617.

115. Citarella A, Scala A, Piperno A, Micale N. SARS-CoV-2 M^pro: a potential target for peptidomimetics and small-molecule inhibitors. *Biomolecules* 2021;**11**:607.

116. Cho SM, White N, Premraj L, Battaglini D, Fanning J, Suen J, et al. Neurological manifestations of COVID-19 in adults and children. *Brain* 2023;**146**:1648−61.

117. Schechter I, Berger A. On the size of the active site in proteases. I. Papain. *Biochem Biophys Res Commun* 1967;**27**:157−62.

118. Liu L, Liu R, Yang X, Hou X, Fang H. Design, synthesis and biological evaluation of tyrosine derivatives as Mcl-1 inhibitors. *Eur J Med Chem* 2020;**191**:112142.

119. Liu R, Liu L, Liu T, Yang X, Wan Y, Fang H. Discovery and development of substituted tyrosine derivatives as Bcl-2/Mcl-1 inhibitors. *Bioorg Med Chem* 2018;**26**:4907−15.

120. Balbach J, Stubbs MT. Coupling proteins, with deadly consequences. *Science* 2023;**381**:126−7.

121. Orta AK, Riera N, Li YE, Tanaka S, Yun HG, Klaic L, et al. The mechanism of the phage-encoded protein antibiotic from ΦX174. *Science* 2023;**381**:eadg9091.

122. Bernhardt TG, Roof WD, Young R. Genetic evidence that the bacteriophage φX174 lysis protein inhibits cell wall synthesis. *Proc Natl Acad Sci U S A* 2000;**97**:4297−302.

123. Mendel S, Holbourn JM, Schouten JA, Bugg TDH. Interaction of the transmembrane domain of lysis protein E from bacteriophage φX174 with bacterial translocase MraY and peptidyl-prolyl isomerase SlyD. *Microbiology* 2006;**152**:2959−67.

124. Whitby LR, Boger DL. Comprehensive peptidomimetic libraries targeting protein−protein interactions. *Acc Chem Res* 2012;**45**:1698−709.

125. Cummings CG, Hamilton AD. Disrupting protein−protein interactions with non-peptidic, small molecule α-helix mimetics. *Curr Opin Chem Biol* 2010;**14**:341−6.

126. Scott DE, Bayly AR, Abell C, Skidmore J. Small molecules, big targets: drug discovery faces the protein−protein interaction challenge. *Nat Rev Drug Discov* 2016;**15**:533−50.

127. Jenkins FJ, Rowe DT, Rinaldo CR. Herpesvirus infections in organ transplant recipients. *Clin Vaccin Immunol* 2003;**10**:1−7.

128. Tong L, Qian C, Massariol MJ, Déziel R, Yoakim C, Lagacé L. Conserved mode of peptidomimetic inhibition and substrate recognition of human cytomegalovirus protease. *Nat Struct Biol* 1998;**5**:819−26.

129. Shieh H-S, Kurumbail RG, Stevens AM, Stegeman RA, Sturman EJ, Pak JY, et al. Three-dimensional structure of human cytomegalovirus protease. *Nature* 1996;**383**:279−82.

130. Khayat R, Batra R, Qian C, Halmos T, Bailey M, Tong L. Structural and biochemical studies of inhibitor binding to human cytomegalovirus protease. *Biochemistry* 2003;**42**:885−91.

131. Goto Y, Suga H. The RaPID platform for the discovery of pseudonatural macrocyclic peptides. *Acc Chem Res* 2021;**54**:3604−17.

132. Ishizawa T, Kawakami T, Reid PC, Murakami H. TRAP Display: a high-speed selection method for the generation of functional polypeptides. *J Am Chem Soc* 2013;**135**:5433−40.

133. Goto Y, Katoh T, Suga H. Flexizymes for genetic code reprogramming. *Nat Protoc* 2011;**6**:779−90.

134. Wang XS, Chen PHC, Hampton JT, Tharp JM, Reed CA, Das SK, et al. A genetically encoded, phage-displayed cyclic-peptide library. *Angew Chem Int Ed* 2019;**58**:15904−9.

135. Sohrabi C, Foster A, Tavassoli A. Methods for generating and screening libraries of genetically encoded cyclic peptides in drug discovery. *Nat Rev Chem* 2020;**4**:90−101.

136. Ogilvie W, Bailey M, Poupart M-A, Bhavsar A, Abraham A, Bonneau P, et al. Peptidomimetic inhibitors of the human cytomegalovirus protease. *J Med Chem* 1997;**40**:4113−35.

137. Swain SP, Mohanty S. Imidazolidinones and imidazolidine-2,4-diones as antiviral agents. *ChemMedChem* 2019;**14**:291−302.

138. Campos IT, Souza TA, Torquato RJ, De Marco R, Tanaka-Azevedo AM, Tanaka AS, et al. The kazal-type inhibitors infestins 1 and 4 differ in specificity but are similar in three-dimensional structure. *Acta Crystallogr D Biol Crystallogr* 2012;**68**:695−702.

139. da Cunha Morales Alvares A, Schwartz EF, Amaral NO, Trindade NR, Pedrino GR, Silva LP, et al. Bowman-Birk protease inhibitor from vigna unguiculata seeds enhances the action of bradykinin-related peptides. *Molecules* 2014;**19**:17536−58.

140. Wang L, Zhao F, Li M, Zhang H, Gao Y, Cao P, et al. Conformational changes of rBTI from buckwheat upon binding to trypsin: implications for the role of the P(8)′ residue in the potato inhibitor I family. *PLoS One* 2011;**6**:e20950.

141. Schmidt AE, Chand HS, Cascio D, Kisiel W, Bajaj SP. Crystal structure of kunitz domain 1 (KD1) of tissue factor pathway inhibitor-2 in complex with trypsin. Implications for KD1 specificity of inhibition. *J Biol Chem* 2005;**280**:27832−8.

142. Zhou D, Lobo YA, Batista IF, Marques-Porto R, Gustchina A, Oliva ML, et al. Crystal structures of a plant trypsin inhibitor from enterolobium contortisiliquum (EcTI) and of its complex with bovine trypsin. *PLoS One* 2013;**8**:e62252.

143. Liebscher S, Schopfel M, Aumuller T, Sharkhuukhen A, Pech A, Hoss E, et al. N-terminal protein modification by substrate-activated reverse proteolysis. *Angew Chem Int Ed Engl* 2014;**53**:3024−8.

144. Ko E, Raghuraman A, Perez LM, Ioerger TR, Burgess K. Exploring key orientations at protein−protein interfaces with small molecule probes. *J Am Chem Soc* 2013;**135**:167−73.

145. Xin D, Holzenburg A, Burgess K. Small molecule probes that perturb a protein−protein interface in antithrombin. *Chem Sci* 2014;**5**:4914−21.

146. Jabeen A, Vijayram R, Ranganathan S. A two-stage computational approach to predict novel ligands for a chemosensory receptor. *Curr Res Struct Biol* 2020;**2**:213−21.

147. Case DA, Cheatham 3rd TE, Darden T, Gohlke H, Luo R, Merz Jr KM, et al. The Amber biomolecular simulation programs. *J Comput Chem* 2005;**26**:1668−88.

148. Greener JG, Kandathil SM, Moffat L, Jones DT. A guide to machine learning for biologists. *Nat Rev Mol Cel Biol* 2021;**23**:40−55.

149. Deo RC. Machine learning in medicine. *Circulation* 2015;**132**:1920−30.

150. Wang X, Du Z, Guo Y, Zhong J, Song K, Wang J, et al. Computer-aided molecular design and optimization of potent inhibitors disrupting APC−Asef interaction. *Acta Pharm Sin B* 2024;**14**:2631−45.

151. Xu Z, Wang X, Zeng S, Ren X, Yan Y, Gong Z. Applying artificial intelligence for cancer immunotherapy. *Acta Pharm Sin B* 2021;**11**:3393−405.

152. Lutz ID, Wang S, Norn C, Courbet A, Borst AJ, Zhao YT, et al. Top-down design of protein architectures with reinforcement learning. *Science* 2023;**380**:266−73.

153. Gross JD, Zhou Y, Barak LS, Caron MG. Ghrelin receptor signaling in health and disease: a biased view. *Trends Endocrinol Metab* 2023;**34**:106−18.

154. Wang W, Tao YX. Ghrelin receptor mutations and human obesity. *Prog Mol Biol Transl Sci* 2016;**140**:131−50.

155. Poher AL, Tschop MH, Muller TD. Ghrelin regulation of glucose metabolism. *Peptides* 2018;**100**:236−42.

156. Jin C, Luo X, Li X, Zhou R, Zhong Y, Xu Z, et al. Positron emission tomography molecular imaging-based cancer phenotyping. *Cancer* 2022;**128**:2704−16.

157. Donegani MI, Ferrarazzo G, Marra S, Miceli A, Raffa S, Bauckneht M, et al. Positron emission tomography-based response to target and immunotherapies in oncology. *Med Kaunas* 2020;**56**:373.

158. Tarkin JM, Corovic A, Wall C, Gopalan D, Rudd JH. Positron emission tomography imaging in cardiovascular disease. *Heart* 2020;**106**:1712−8.

159. Hanrahan P, Bell J, Bottomley G, Bradley S, Clarke P, Curtis E, et al. Substituted azaquinazolinones as modulators of GHSr-1a for the treatment of type II diabetes and obesity. *Bioorg Med Chem Lett* 2012;**22**:2271−8.

160. Moulin A, Brunel L, Boeglin D, Demange L, Ryan J, M'Kadmi C, et al. The 1,2,4-triazole as a scaffold for the design of ghrelin receptor ligands: development of JMV 2959, a potent antagonist. *Amino Acids* 2013;**44**:301−14.

161. Hou J, Kovacs MS, Dhanvantari S, Luyt LG. Development of candidates for positron emission tomography (PET) imaging of ghrelin

receptor in disease: design, synthesis, and evaluation of fluorine-bearing quinazolinone derivatives. *J Med Chem* 2018;**61**:1261−75.

162. M'Kadmi C, Cabral A, Barrile F, Giribaldi J, Cantel S, Damian M, et al. N-terminal liver-expressed antimicrobial peptide 2 (LEAP2) region exhibits inverse agonist activity toward the ghrelin receptor. *J Med Chem* 2019;**62**:965−73.

163. Buhlmann S, Reymond JL. ChEMBL-likeness score and database GDBChEMBL. *Front Chem* 2020;**8**:46.

164. Papadatos G, Overington JP. The ChEMBL database: a taster for medicinal chemists. *Future Med Chem* 2014;**6**:361−4.

165. Herrera-Acevedo C, Perdomo-Madrigal C, Herrera-Acevedo K, Coy-Barrera E, Scotti L, Scotti MT. Machine learning models to select potential inhibitors of acetylcholinesterase activity from sistematx: a natural products database. *Mol Divers* 2021;**25**:1553−68.

166. Handelman GS, Kok HK, Chandra RV, Razavi AH, Lee MJ, Asadi H. eDoctor: machine learning and the future of medicine. *J Intern Med* 2018;**284**:603−19.

167. Uddin S, Khan A, Hossain ME, Moni MA. Comparing different supervised machine learning algorithms for disease prediction. *BMC Med Inform Decis Mak* 2019;**19**:281.

168. Kaneko H. Molecular descriptors, structure generation, and inverse QSAR/QSPR based on SELFIES. *ACS Omega* 2023;**8**:21781−6.

169. Miljkovic F, Rodriguez-Perez R, Bajorath J. Machine learning models for accurate prediction of kinase inhibitors with different binding modes. *J Med Chem* 2020;**63**:8738−48.

170. Siramshetty VB, Chen Q, Devarakonda P, Preissner R. The Catch-22 of predicting hERG blockade using publicly accessible bioactivity data. *J Chem Inf Model* 2018;**58**:1224−33.

171. Wojtuch A, Jankowski R, Podlewska S. How can SHAP values help to shape metabolic stability of chemical compounds?. *J Cheminform* 2021;**13**:74.

172. Lundberg SM, Lee SI. A unified approach to interpreting model predictions. In: Guyon I, Luxburg UV, Bengio S, Wallach H, Fergus R, Vishwanathan SVN, et al., editors. *Advances in neural information processing systems 30 (NIPS 2017)*. New York: Curran Associates; 2017. p. 4765−74.

173. Zhong S, Guan X. Count-based morgan fingerprint: a more efficient and interpretable molecular representation in developing machine learning-based predictive regression models for water contaminants' activities and properties. *Environ Sci Technol* 2023;**57**:18193−202.

174. Bu Y, Ma J, Bei J, Wang S. Surface modification of aliphatic polyester to enhance biocompatibility. *Front Bioeng Biotechnol* 2019;**7**:98.

175. Shiimura Y, Horita S, Hamamoto A, Asada H, Hirata K, Tanaka M, et al. Structure of an antagonist-bound ghrelin receptor reveals possible ghrelin recognition mode. *Nat Commun* 2020;**11**:4160.

176. Anerillas C, Mazan-Mamczarz K, Herman AB, Munk R, Lam KG, Calvo-Rubio M, et al. The YAP−TEAD complex promotes senescent cell survival by lowering endoplasmic reticulum stress. *Nat Aging* 2023;**3**:1237−50.

177. Ong YT, Andrade J, Armbruster M, Shi C, Castro M, Costa ASH, et al. A YAP/TAZ-TEAD signalling module links endothelial nutrient acquisition to angiogenic growth. *Nat Metab* 2022;**4**:672−82.

178. Sun Y, Hu L, Tao Z, Jarugumilli GK, Erb H, Singh A, et al. Pharmacological blockade of TEAD−YAP reveals its therapeutic limitation in cancer cells. *Nat Commun* 2022;**13**:6744.

179. Samji P, Rajendran MK, Warrier VP, Ganesh A, Devarajan K. Regulation of hippo signaling pathway in cancer: a microrna perspective. *Cell Signal* 2021;**78**:109858.

180. Pan D. The hippo signaling pathway in development and cancer. *Dev Cel* 2010;**19**:491−505.

181. Harvey KF, Zhang X, Thomas DM. The hippo pathway and human cancer. *Nat Rev Cancer* 2013;**13**:246−57.

182. Johnson R, Halder G. The two faces of hippo: targeting the hippo pathway for regenerative medicine and cancer treatment. *Nat Rev Drug Discov* 2014;**13**:63−79.

183. Moon S, Yeon Park S, Woo Park H. Regulation of the hippo pathway in cancer biology. *Cell Mol Life Sci* 2018;**75**:2303−19.

184. Calses PC, Crawford JJ, Lill JR, Dey A. Hippo pathway in cancer: aberrant regulation and therapeutic opportunities. *Trends Cancer* 2019;**5**:297−307.

185. Schmelzle T, Chapeau E, Bauer D, Chene P, Faris J, Fernandez C, et al. IAG933, a selective and orally efficacious YAP1/WWTR1(TAZ)−panTEAD protein−protein interaction inhibitor with pre-clinical activity in monotherapy and combinations [abstract]. In: Schmelzle T, Chapeau E, Bauer D, Chene P, Faris J, Fernandez C, et al., editors. Proceedings of the American association for cancer research annual meeting 2023. 2023 Apr 14−19. Orlando, FL. Philadelphia (PA): AACR; 2023. LB319.

186. Sturbaut M, Bailly F, Coevoet M, Sileo P, Pugniere M, Liberelle M, et al. Discovery of a cryptic site at the interface 2 of TEADtowards a new family of YAP/TAZ-TEAD inhibitors. *Eur J Med Chem* 2021;**226**:113835.

187. Smith SA, Sessions RB, Shoemark DK, Williams C, Ebrahimighaei R, McNeill MC, et al. Antiproliferative and antimigratory effects of a novel YAP−TEAD interaction inhibitor identified using *in silico* molecular docking. *J Med Chem* 2019;**62**:1291−305.

188. Li Z, Zhao B, Wang P, Chen F, Dong Z, Yang H, et al. Structural insights into the YAP and TEAD complex. *Genes Dev* 2010;**24**:235−40.

189. Tian W, Yu J, Tomchick DR, Pan D, Luo X. Structural and functional analysis of the YAP-binding domain of human tead2. *Proc Natl Acad Sci U S A* 2010;**107**:7293−8.

190. Chen L, Chan SW, Zhang X, Walsh M, Lim CJ, Hong W, et al. Structural basis of YAP recognition by tead4 in the hippo pathway. *Genes Dev* 2010;**24**:290−300.

191. Wang P, Wang M, Hu Y, Chen J, Cao Y, Liu C, et al. Isorhapontigenin protects against doxorubicin-induced cardiotoxicity *via* increasing YAP1 expression. *Acta Pharm Sin B* 2021;**11**:680−93.

192. Mesrouze Y, Gubler H, Villard F, Boesch R, Ottl J, Kallen J, et al. Biochemical and structural characterization of a peptidic inhibitor of the YAP:TEAD interaction that binds to the alpha-helix pocket on TEAD. *ACS Chem Biol* 2023;**18**:643−51.

193. Chang L, Azzolin L, Di Biagio D, Zanconato F, Battilana G, Lucon Xiccato R, et al. The SWI/SNF complex is a mechanoregulated inhibitor of YAP and TAZ. *Nature* 2018;**563**:265−9.

194. Furet P, Salem B, Mesrouze Y, Schmelzle T, Lewis I, Kallen J, et al. Structure-based design of potent linear peptide inhibitors of the YAP−TEAD protein−protein interaction derived from the YAP omega-loop sequence. *Bioorg Med Chem Lett* 2019;**29**:2316−9.

195. Friesner RA, Banks JL, Murphy RB, Halgren TA, Klicic JJ, Mainz DT, et al. Glide: a new approach for rapid, accurate docking and scoring. 1. Method and assessment of docking accuracy. *J Med Chem* 2004;**47**:1739−49.

196. Case DA, Aktulga HM, Belfon K, Ben-Shalom I, Brozell SR, Cerutti DS, et al. *Amber 2021*. San Francisco: University of California; 2021.

197. Salomon-Ferrer R, Gotz AW, Poole D, Le Grand S, Walker RC. Routine microsecond molecular dynamics simulations with amber on GPUs. 2. Explicit solvent particle mesh ewald. *J Chem Theor Comput* 2013;**9**:3878−88.

198. Sindhikara DJ, Hirata F. Analysis of biomolecular solvation sites by 3D-RISM theory. *J Phys Chem B* 2013;**117**:6718−23.

199. Tian C, Kasavajhala K, Belfon KAA, Raguette L, Huang H, Migues AN, et al. Ff19sb: amino-acid-specific protein backbone parameters trained against quantum mechanics energy surfaces in solution. *J Chem Theor Comput* 2020;**16**:528−52.

200. Hornak V, Abel R, Okur A, Strockbine B, Roitberg A, Simmerling C. Comparison of multiple Amber force fields and development of improved protein backbone parameters. *Proteins* 2006;**65**:712−25.

201. Jorgensen WL, Chandrasekhar J, Madura JD, Impey RW, Klein ML. Comparison of simple potential functions for simulating liquid water. *J Chem Phys* 1983;**79**:926−35.

202. Velez-Vega C, McKay DJ, Aravamuthan V, Pearlstein R, Duca JS. Time-averaged distributions of solute and solvent motions: exploring proton wires of GFP and PfM2DH. *J Chem Inf Model* 2014;**54**:3344−61.

203. Velez-Vega C, McKay DJ, Kurtzman T, Aravamuthan V, Pearlstein RA, Duca JS. Estimation of solvation entropy and enthalpy via analysis of water oxygen-hydrogen correlations. *J Chem Theor Comput* 2015;**11**:5090−102.

204. Lee TS, Allen BK, Giese TJ, Guo Z, Li P, Lin C, et al. Alchemical binding free energy calculations in AMBER20: advances and best practices for drug discovery. *J Chem Inf Model* 2020;**60**:5595−623.

205. Mermelstein DJ, Lin C, Nelson G, Kretsch R, McCammon JA, Walker RC. Fast and flexible GPU accelerated binding free energy calculations within the amber molecular dynamics package. *J Comput Chem* 2018;**39**:1354−8.

206. Lee TS, Hu Y, Sherborne B, Guo Z, York DM. Toward fast and accurate binding affinity prediction with pmemdGTI: an efficient implementation of GPU-accelerated thermodynamic integration. *J Chem Theor Comput* 2017;**13**:3077−84.

207. Hagberg A, Swart P, S Chult D. *Exploring network structure, dynamics, and function using NetworkX*. Los Alamos, NM, USA: Los Alamos National Lab.(LANL); 2008.